NASA MEMO 2-11-59L

NASA

MEMORANDUM

AN INVESTIGATION OF THE PERFORMANCE OF

VARIOUS REACTION CONTROL DEVICES

By Paul A. Hunter

Langley Research Center
Langley Field, Va.

NATIONAL AERONAUTICS AND SPACE ADMINISTRATION

WASHINGTON

March 1959

NATIONAL AERONAUTICS AND SPACE ADMINISTRATION

MEMORANDUM 2-11-59L

AN INVESTIGATION OF THE PERFORMANCE OF VARIOUS REACTION CONTROL DEVICES

By Paul A. Hunter

SUMMARY

An investigation of a number of small-scale reaction control devices in still air with both subsonic and supersonic internal flows has shown that lateral forces approaching 70 percent of the resultant force of the undeflected jet can be obtained. These results were obtained with a tilted extension at a deflection of 40°. The tests of tilted extensions indicated an optimum length-to-diameter ratio of approximately 0.75 to 1.00, dependent upon the deflection angle. For the two geometric types of spoiler tabs tested, blockage-area ratio appears to be the only variable affecting the lateral force developed. Usable values of lateral force were developed by the full-eyelid type of device with reasonably small losses in thrust and weight flow. Somewhat larger values of lateral force were developed by injecting a secondary flow normal to the primary jet, but for the conditions of these tests the losses in thrust and weight flow were large. Relatively good agreement with other investigations was obtained for several of the devices. The agreement of the present results with those of an investigation made with larger-scale equipment indicates that Reynolds number may not be critical for these tests. Inasmuch as the effects of external flow could influence the performance and other factors affecting the choice of a reaction control for a specific use, it would appear desirable to make further tests of the devices described in this report in the presence of external flow.

INTRODUCTION

The increasing development of vertical-take-off-and-landing aircraft and high-altitude missiles has pointed to the need for additional research on reaction controls for vehicles operating under conditions of low dynamic pressure.

Most of the investigations reported so far have been of single devices or of a series of devices tested only with a supersonic jet (refs. 1 to 6). An investigation of a number of jet deflectors up to a primary-nozzle pressure ratio of 3.0 is described in reference 7. For

the investigation of reference 7 emphasis was placed on devices which could be adapted to conventional turbojet engines.

The present investigation covers a range of configurations tested in still air utilizing both subsonic and supersonic internal flow. Small-scale devices were tested by the blowdown technique over nozzle total-pressure-ratio ranges from approximately 1.3 to 6.5. The devices, as tested, do not necessarily represent practical configurations but demonstrate the performance obtained with certain basic types of devices.

The results from each of the devices are presented separately, with a comparison of the devices of this investigation and other investigations following the presentation of results.

SYMBOLS

A_b/A	ratio of blocked exit area to total exit area for spoiler tabs
d	nozzle exit diameter, in.
F_R	resultant force, lb
F_X	longitudinal force, lb
F_Y	lateral force, lb
g	acceleration of gravity, ft/sec^2
l	mean length of deflector, in.
p	atmospheric static pressure, lb/sq ft
p_t	total pressure, lb/sq ft
r	radius
w	jet-exhaust weight flow, lb/sec
w_s	secondary air weight flow, lb/sec
V	velocity, ft/sec
δ	mechanical deflection angle, deg

Superscript:

* quantity measured with no deflection device in place

APPARATUS

The apparatus used (fig. 1) consisted primarily of an air storage tank and associated piping which terminated in a nozzle which produced the simulated jet exhaust. The tank had a volume of 82.8 cu ft. Air was supplied to the tank from a 200-pound-per-square-inch utility system through a variable-pressure regulating valve. Air from the tank entered the 2-inch-internal-diameter piping through a nozzle having a double-radius convergent profile to promote low-turbulence entry. Downstream of this nozzle was a manually operated, quick-acting ball valve which, when open, produced no area reduction to flow. The loop and flexible connections in the piping were included to reduce restraint and pressure effects in the force measurements. For some of the tests (pneumatic diverter) an additional (secondary) air supply was required. This supply was obtained from the already mentioned 200-pound-per-square-inch utility system tapped off upstream of the regulating valve. Flow in this system was controlled by a ball valve similar to that in the primary system. Both systems were also provided with gate-type shut-off valves upstream of all other equipment. Two interchangeable nozzles were used to produce the simulated jet exhaust. The subsonic and supersonic nozzles are shown in figure 2. Where applicable, the effect of devices on the flow with the supersonic nozzle is discussed in connection with the individual devices. Both nozzles had exit diameters of 1.125 inches and wall thicknesses at the exit of 0.063 inch. The throat diameter of the supersonic nozzle was 1.037 inches (expansion ratio, 1.176).

TESTS AND DEFLECTION DEVICES

Each test was of the blowdown type and was conducted between two predetermined pressures. The air temperature in the tank was allowed to stabilize before the beginning of each test. During each blowdown test continuous measurements were made of tank air temperature and pressure, tank nozzle-throat static pressure, total pressure just upstream of the exit nozzle, longitudinal and lateral forces, and moment. The atmospheric pressure was determined for each test by an indicating microbarograph. The air weight flow was computed from the first three quantities, and the nozzle total-pressure ratio was computed from the exit-nozzle total pressure and the atmospheric pressure. The longitudinal and lateral forces and moment were measured with a strain-gage balance. Each deflection device was tested with the subsonic nozzle over a nozzle

total-pressure-ratio range of from approximately 1.3 to 2.6 and with the supersonic nozzle over nozzle total-pressure-ratio ranges of from approximately 1.9 to 4.0 and from approximately 3.4 to 6.5. In addition, a pneumatic diverter device was tested over a range of secondary air weight flows. The secondary air weight flow was determined by use of an A.S.M.E. sharp-edged orifice.

A representative sampling of the deflection devices tested is shown in the photograph of figure 2(a) and the sketches of figure 2(b). Most of the devices were designed to fit on the nozzles with no change in internal area as the flow passed from the nozzle into the device. The family of devices designated tilted extension, a few of which are shown in the center of figure 2(a), were tested over a tilt-angle range of from 0° to 40° and a range of the ratio of mean length to exit diameter of from 0.25 to 3.0.

The devices designated spoiler tabs were tested in two series: (1) segment type, full chord with the height of the spoiler varied, and (2) tooth type, constant height with the width of the spoiler varied. The lips of the tabs were beveled in order to produce a sharp edge at the upstream side.

For the device labeled the asymmetric inducer, half of the annular opening was sealed with modeling clay to produce an asymmetric external induced flow when the device was in use. Tests were also made without the clay seal for comparative purposes. The supporting portions of the spoiler tab and asymmetric inducer devices fitted on the outside of the nozzle and produced the effect of increased nozzle wall thickness insofar as external flows and boattailing effects were concerned. The split extension was a tubular extension, one side of which could be positioned over an approximate angular range of from 0° to 16° with respect to the longitudinal axis. The ratio of length to internal diameter of this device was 2.0.

The single eyelid is shown mounted on an extension. The eyelid itself was of elliptical form with a 60° included angle and could be positioned over an angular range of from 38.8° to 90° from the plane normal to the longitudinal axis. In the 38.8° position, the downstream edge of the eyelid was coincident with the projection of the inner surface of the extension on which it was mounted.

At the upper right in figure 2(a) is shown the full eyelid mounted on its own nozzle. The internal surface of the eyelid was spherical and the exit diameter was 1.125 inches. The eyelid could be positioned over a range of angles of $\pm 15^{\circ}$ from a position normal to the longitudinal axis. The nozzle on which it was mounted was a convergent nozzle having a minimum internal diameter of 1.378 inches. This difference in diameters

was necessary to permit retaining constant exit area throughout the eyelid deflection range. This device simulates an afterburner nozzle which is swiveled to deflect the jet flow.

At the left in the photograph (fig. 2(a)) is shown the pneumatic diverter, which consisted of an annular passage surrounding the primary jet, divided into four 90° sectors, each of which had an air inlet tube. Each sector exhausted into the primary jet normal to the longitudinal axis through a slot 1/16 inch wide extending through one-quarter of the internal circumference. For these tests, only one of the four sectors was used. The pneumatic diverter was tested with and without a set of 90° turning vanes. (See fig. 2.) When in place, the upstream lip of the first vane was one nozzle diameter downstream of the diverter exit. The six vanes had an internal diameter of $1\frac{1}{8}$ inches and were spaced at $\frac{9}{32}$-inch intervals.

Tests were also made with no deflection device in place. From these tests were obtained the data with which the deflected-jet data are compared, the tank nozzle-discharge coefficients, and the tare corrections to the lateral force and moment data.

RESULTS AND DISCUSSION

The results of this investigation have been nondimensionalized insofar as is possible. Figure 3 represents a typical vector diagram of the forces developed by a reaction control of the type discussed herein. The lateral-force parameter F_Y/F_R^* represents the ratio of the lateral force developed to the resultant force of the undeflected jet and permits estimation of the lateral force developed from known thrust values. F_R/F_R^* is the ratio of the resultant force to the resultant force of the undeflected jet and may be considered as the efficiency of the deflection process. For the vectors shown in figure 3, F_R is less than F_R^*. The portion of the original thrust force acting along the undeflected axis F_X can be determined by $F_R \cos \theta$ where θ is the angle whose sine is the ratio of the lateral-force parameter to the resultant-force parameter. The effect of deflection on engine operation is indicated by the weight-flow ratio w/w^*. Figure 4 shows the magnitudes of resultant force and weight flow of the undeflected jet with which the data from the deflected jet were compared. The estimated extrapolations of the curves for the subsonic nozzle are used for only one device and are discussed later. Calculations of theoretical resultant force based on measured weight flow indicated nozzle efficiencies of the order of 95 to 100 percent. The weight flow and resultant force were not reduced to

standard conditions since the atmospheric temperatures and pressures encountered during the tests were so near standard as to make negligible any differences in weight flow and resultant force.

In the following discussion, the results from each of the devices is presented separately, with a comparison of the devices following the presentation of results.

Tilted Extensions

Lateral-force parameter F_Y/F_R^* (fig. 5(a)).- The data show that at supercritical nozzle total-pressure ratios an optimum value of l/d exists which varies between 0.75 and 1.00 with deflection angle. This effect is more pronounced for the supersonic nozzle than for the subsonic nozzle.

For the supersonic nozzle, the magnitude of F_Y/F_R^* seems to be practically independent of nozzle total-pressure ratio except for the lowest pressure ratio and small values of l/d. For a given value of l/d, F_Y/F_R^* increases linearly with increasing δ. Peak values of F_Y/F_R^* approaching 0.7 were obtained at $\delta = 40^\circ$. For the subsonic nozzle the variation of F_Y/F_R^* with δ becomes less linear at the larger values of δ. The symbols were omitted from the figure for reasons of clarity.

Resultant-force parameter F_R/F_R^* (fig. 5(b)).- The data show that the resultant-force parameter experiences a loss which increases with δ and decreases with increasing pressure ratio for the subsonic nozzle. For the supersonic nozzle, pressure ratio seems to have little or no effect. At l/d of 1.5 and smaller, there is an apparent recovery at $\delta = 40^\circ$ which varies with pressure ratio. This variation does not follow a consistent pattern, however.

Weight-flow ratio w/w^* (fig. 5(c)).- As would be expected, there was no effect of δ or l/d on weight-flow ratio for the supersonic nozzle. With the subsonic nozzle the weight-flow ratio varies with δ and p_t/p in the same manner as the resultant-force parameter. For a given δ and pressure ratio, the greatest loss occurs at an l/d about 0.50 to 0.75, although the variation with l/d is not large. The basic flow equation

$$F_R = \frac{wV}{g} \tag{1}$$

described the relation between resultant force and weight flow and is used again later to explain some unusual variations of these quantities.

Spoiler Tabs

Lateral-force parameter F_Y/F_R^* (fig. 6(a)).- The magnitude of F_Y/F_R^* increases with increasing blockage-area ratio and reaches a maximum at a blockage-area ratio of about 0.2. Within each flow regime the magnitude of F_Y/F_R^* decreases with increasing pressure ratio. For these tests, no significant effect of blockage type (segment or tooth) was apparent although the range of blockage area for the tooth type was relatively limited.

Resultant-force parameter F_R/F_R^* (fig. 6(b)).- For the subsonic nozzle the resultant-force parameter experiences a loss which increases with blockage-area ratio regardless of spoiler type. With the supersonic nozzle there is little or no loss until a blockage ratio of about 0.15 is exceeded. The loss then increases sharply with increasing blockage-area ratio but at a given value of A_b/A decreases as the pressure ratio is increased. These losses are a direct result of the loss in weight flow which is discussed in the following section.

Weight-flow ratio w/w^* (fig. 6(c)).- For the subsonic nozzle the data show a decrease in weight-flow ratio with increasing blockage-area ratio. For the supersonic nozzle there is no effect of blockage-area ratio until a value of A_b/A of about 0.15 is exceeded, at which point the weight flow begins to drop off rapidly with increasing values of A_b/A. The loss in weight flow indicates that for values of $A_b/A > 0.15$ the flow is no longer supersonic because the exit area has become less than the nozzle throat area. The expansion ratio for this nozzle was 1.176, the reciprocal of which is 0.85.

The values of $w/w^* > 1.0$ are believed to be the result of experimental error, the difference in absolute magnitude of weight flow corresponding to 4 percent of the undeflected weight flow at $p_t/p = 2.5$ being about 0.027 pound per second. (See fig. 4.) As was the case with F_Y/F_R^* and F_R/F_R^*, the type of spoiler appeared to have no effect on the weight-flow ratio.

Asymmetrical Inducer

The lateral forces developed with the asymmetrical inducer were so low as to be within the scatter band, so no results are given. Insofar

as these tests are concerned, this device appears to be useless as a reaction control. External flow might produce some beneficial effects, however.

Split Extensions

Lateral-force parameter F_Y/F_R^* (fig. 7).- The variation of F_Y/F_R^* with δ is linear for the subsonic nozzle, with a slight decrease in slope indicated for increasing pressure ratio. This variation appears nonlinear for the supersonic nozzle, with little effect of pressure ratio except at the highest pressure ratio shown.

Resultant-force parameter F_R/F_R^* (fig. 7).- The loss in resultant force with δ is small and relatively free of pressure-ratio effect for the subsonic nozzle. With the supersonic nozzle the loss in the resultant-force parameter appears to vary inversely with pressure ratio.

Weight-flow ratio w/w^* (fig. 7).- There is no effect of δ on weight-flow ratio for either nozzle. The weight-flow ratios greater than 1 shown for the subsonic nozzle are believed to be a result of experimental error due to the low absolute magnitude of the flow rate at these pressure ratios. (See fig. 4.)

Full Eyelid

Lateral-force parameter F_Y/F_R^* (fig. 8).- The variation of F_Y/F_R^* with δ is fairly linear through the range of deflection angles tested. Pressure ratio appears to have no effect on F_Y/F_R^*. Inasmuch as the nozzle on which the full eyelid was mounted was a simple convergent nozzle, subsonic values of undeflected thrust and weight flow were used in converting these data to nondimensional form. For the higher pressure ratios where no experimental values of undeflected thrust and weight flow were obtained, estimated extrapolations of these data were used. (See fig. 4.)

Resultant-force parameter F_R/F_R^* (fig. 8).- At the lower pressure ratios, increasing pressure ratio appears to have a beneficial effect on F_R/F_R^*, but this effect becomes negligible at the higher pressure ratios. No concise effect of δ on F_R/F_R^* is apparent.

Weight-flow ratio w/w^* (fig. 8).- The effects of pressure ratio and δ on w/w^* are quite similar to those on F_R/F_R^*. The effect of pressure ratio seems to disappear at a lower value of p_t/p for the

weight-flow ratio than for F_R/F_R^*. Even at the highest pressure ratio tested, a small loss of weight-flow ratio at $\delta = 0$ was evident. The reason for the loss in F_R/F_R^* and w/w^* at $\delta = 0$ would appear to be the sudden contraction at the eyelid exit. This contraction did not exist with the other devices. (See fig. 2.)

Single Eyelid

Lateral-force parameter F_Y/F_R^* (fig. 9(a)).- F_Y/F_R^* increases with δ in a nonlinear manner. As was pointed out in the description of the eyelid, the value of $\delta = 38.8^\circ$ is the deflection at which the downstream lip of the eyelid just begins to project into the edge of the jet. The rate of change of F_Y/F_R^* with δ reflects the rate of reduction of effective nozzle exit area with δ. The reduction of effective nozzle exit area decreases the thrust, and this reduction is discussed in the section on weight-flow ratio. Increasing pressure ratio appears to increase the effectiveness slightly for the subsonic nozzle but to have no effect on the supersonic nozzle.

The ratio of the measured moment about the balance center to the lateral force indicated that the lateral force was developed at a point somewhat upstream of the lip of the eyelid but downstream of the pivot axis of the eyelid.

Resultant-force parameter F_R/F_R^* (fig. 9(b)).- There is a loss in the resultant-force parameter at all pressure ratios above a δ of about 50° which varies inversely with pressure ratio with the subsonic nozzle. The effect of pressure ratio is small, however. With the supersonic nozzle there is no clearcut variation with pressure ratio. The magnitude of the losses at a given δ was lower for the supersonic nozzle than for the subsonic nozzle.

Weight-flow ratio w/w^* (fig. 9(c)).- With the subsonic nozzle, there was a loss in weight flow with δ, beginning at about 50° as with F_R/F_R^*. Because the variation of the two quantities with δ is quite similar, their interdependence as shown by equation (1) is indicated. The reduction of effective nozzle exit area with increasing δ causes a reduction in weight flow, which in turn causes a reduction in the resultant force. With the supersonic nozzle, however, the weight-flow ratio shows no loss until a δ of 75° is exceeded. This indicates that the eyelid is restricting the exit area at these larger deflections to such an extent that the flow is probably no longer supersonic. In this deflection range the eyelid apparently acts much as the spoiler tabs. Below 75°, figure 9(b) shows some loss in resultant force, but

since there is no loss in weight flow over this range, equation (1) shows the loss in F_R/F_R^* must result from a reduction in velocity. The values of weight flow greater than 1 are the result of experimental error, the absolute magnitude of the difference being of the order of 0.025 pound per second. (See fig. 4.)

Pneumatic Diverter

Lateral-force parameter F_Y/F_R^*.- For the diverter without the turning vanes, F_Y/F_R^* increases rapidly with secondary-to-primary weight-flow ratio w_s/w but increases less rapidly at the higher values of w_s/w (fig. 10(a)). The magnitude of F_Y/F_R^* at a given weight-flow ratio drops off slightly with increasing pressure ratio. The effect of adding the 90° vanes was to reduce the lateral-force parameter. This effect of the vanes results from the decrease in thrust which comes about from a symmetrical diversion of a portion of the primary flow and is independent of the amount of secondary flow. The foregoing reasoning is borne out by the loss of thrust at zero secondary flow with vanes on and is discussed in a following section.

Figure 10(b) shows typical examples of the lateral force developed by secondary flow alone and by the primary flow combined with various amounts of secondary flow. The small secondary flows alone produce only small lateral forces, but when combined with the larger primary flow, the larger primary flow is deflected and a much larger lateral force is produced. The force due to the secondary flow alone may have been partially dissipated by the impingement of the flow on the opposite wall of the nozzle. In order to estimate the side force of the secondary flow in an isolated jet, a clay baffle was installed as indicated in figure 2(b) to direct the secondary flow smoothly past the opposite wall of the nozzle. The side force of the secondary flow alone under these conditions was 2.4 times as great as without the baffle. The estimated isolated thrust of the secondary flow is shown in figure 10(b). The side force of the combined primary and secondary flows is seen to be approximately twice the isolated thrust of the secondary flow. As in figure 10(a) the loss in side force caused by the use of the vanes is marked. It would appear that the lateral force developed by the combined flows would, for constant secondary flow, vary directly as the primary weight flow. This fact was borne out for the configuration with no vanes, but for the vanes-on configuration the maximum lateral force was developed at some intermediate value of primary weight flow for a constant secondary weight flow. This phenomenon is believed to be associated with vane diversion.

Some rake measurements made a distance of one nozzle diameter downstream of the undeflected jet indicated that the static pressure of the flow varied with flow conditions between pressures greater than, and less than, atmospheric pressure. The diversion of a portion of the primary flow by the vanes would be expected to be a maximum when the static pressure was greater than atmospheric pressure and minimum or nonexistent when the static pressure was less than atmospheric pressure. The static pressure was generally greater than atmospheric pressure for the portion of the blowdown type of test where the primary weight flows were large and was less than atmospheric pressure for intermediate primary weight flows.

For the no-vane configuration, the ratio of the measured moment to the lateral force indicated the point of application of the lateral force to be at the secondary exit slot. With the vanes on, the point of application moved downstream with increasing secondary flow and with increasing primary flow. Thus, it would appear that the vanes were effective in increasing the moment arm of the control moment but that other losses decreased the overall performance of the vanes-on configuration.

Resultant-force parameter F_R/F_R^* (fig. 10(c)).- With the subsonic nozzle, the resultant-force parameter dropped rapidly with increase in secondary-to-primary weight-flow ratio. The effect of the vanes was to lower the magnitude of F_R/F_R^* at all values of w_s/w. With the supersonic nozzle for the no-vane configuration there was little effect of secondary flow on F_R/F_R^*, but for the vanes-on configuration F_R/F_R^* showed the same trends as for the subsonic nozzle.

Weight-flow ratios w/w^* and w_s/w.- The reason for the loss in F_R/F_R^* can be seen generally by the variation of the primary weight-flow ratio w/w^* in figure 10(d). The data for the subsonic nozzle show a variation in w/w^* similar to that of F_R/F_R^* except that there is no significant loss at $w_s/w = 0$ with vanes on. This is the point which leads to the conclusion that the loss in F_R/F_R^*, and consequently the reduction of F_Y/F_R^* with vanes on, is attributable to symmetrical diversion of the primary flow by the vanes. The data for the supersonic nozzle show a loss in primary weight-flow ratio above $w_s/w = 0.07$ which would indicate the flow is no longer supersonic at secondary flow ratios above this value. Compared with other devices at similar values of F_Y/F_R^*, the losses in primary weight-flow ratio for the subsonic nozzle are quite large. Also, an increase in nozzle total-pressure ratio resulting from secondary flow was noticed during data analysis. These three facts indicate that the static pressure of the secondary jet was acting as a barrier to the primary flow. Thus it would appear that a

secondary flow source having a lower static pressure might have produced equal lateral-force characteristics with smaller losses in F_R/F_R^* and w/w^*.

Comparison of Devices

For the range of variables tested, the tilted extensions produced the largest magnitudes of F_Y/F_R^*. At a deflection of 15°, however, the magnitudes of the lateral-force parameter for the tilted extensions at optimum l/d ratio and the full eyelid are quite similar. With the supersonic nozzle and at higher pressure ratios with the subsonic nozzle, the resultant-force parameter F_R/F_R^* for the full eyelid is more nearly unity and therefore more desirable than the tilted extensions at this same deflection of 15°. On the basis of weight-flow ratio, the full eyelid appears to suffer somewhat in comparison with the tilted extensions. As pointed out in the earlier discussion of the full eyelid, the loss in weight-flow ratio is essentially constant with varying δ; therefore, this loss might be acceptable in certain applications. This loss is a characteristic of the geometry of the eyelid and might be reduced, but not eliminated, by changes in the geometry.

A comparison of the present results for the tilted extensions with those of reference 2 shows general agreement as to the magnitude of side forces. The optimum length-to-diameter ratio for the investigation of reference 2 was 1.2 based on exit diameter compared with the range of 0.75 to 1.00 for the present results. A comparison of the side forces was made for equal tube lengths at $\delta = 40°$, $p_t/p = 3.8$, and at values of l/d (based on exit diameter) equal to 1.67, 1.11, and 0.55. The difference in side force of the results of reference 2 from those of the present investigation at these values of l/d were, respectively, 1.5 percent high, 5.6 percent low, and 1.9 percent low.

A comparison of the tilted extensions with the results of the swivelled tail pipe of reference 7 indicated the side force for the present investigation to be about 10 percent higher at $\delta = 20°$ and $p_t/p = 2.5$. The values of axial thrust agreed to within 4 percent. Reference 7 showed no effect of pressure ratio and did not include an investigation of length-to-diameter ratios. The side forces of the swivelled convergent nozzle of reference 7 were of the order of 10 percent lower than those of the full eyelid of the present investigation.

The investigation of reference 7 was conducted with a basic nozzle diameter of 4 inches compared with $1\frac{1}{8}$ inches for the present investigation. The relatively good agreement of the results of these two investigations indicates that Reynolds number may not be critical for these tests.

While the single eyelid and pneumatic diverter produced lateral-force parameters of reasonable magnitudes, the losses in resultant force and weight-flow ratios make these devices less desirable, at least for the conditions of these tests. For the range of variables tested, the magnitudes of F_Y/F_R^* for the spoiler tabs and split extensions, while low, were very similar. These devices might find application for some types of missiles where only a low degree of maneuverability is required. With the subsonic nozzle, the losses in resultant-force and weight-flow ratios are considerably greater for the spoiler tabs than for the split extensions. With the supersonic nozzle, the resultant-force and weight-flow ratios for the spoiler tabs at blockage-area ratios less than 0.15 compare much more favorably with the split extensions. The lateral-force parameter developed at this blockage-area ratio is a large percentage of the maximum shown in figure 6(a). Thus a split extension or a spoiler tab having a blockage area ratio such that the exit area is equal to or greater than the nozzle throat area might find application for guidance of a rocket missile.

At $\delta = 10^\circ$ a comparison of the split extension (fig. 7) with the tilted extension (fig. 5(a)) shows the side force developed by the tilted extension to be about twice that of the split extension. The lift force developed by the Coanda flap of reference 6 was also roughly twice the side force developed by the split extension of the present investigation at $\delta = 10^\circ$. This discrepancy is probably the result of air entrainment in the split extension since the wall of the split tube did not form a complete side plate. An exact comparison could not be made because of the difference in nozzle geometry. The preceding discussion indicates that at $\delta = 10^\circ$, the forces developed by the tilted extension and the Coanda flap are roughly equal. The Coanda flap reaches an upper limit due to flow separation at a deflection in the range of 20° to 25°, however.

Inasmuch as the effects of external flow could influence the performance and other factors affecting the choice of a reaction control for a specific use, it would appear desirable to make further tests of the devices described herein in the presence of external flow.

CONCLUDING REMARKS

An investigation of a number of small-scale reaction control devices in still air with both subsonic and supersonic internal flows has shown that lateral forces approaching 70 percent of the resultant force of the undeflected jet can be obtained. These results were obtained with a tilted extension at a deflection of 40°. The tests of tilted extensions indicated an optimum ratio of length to exit diameter of approximately 0.75 to 1.00, varying with deflection angle. For the two geometric

types of spoiler tabs tested (segment or tooth), blockage-area ratio appears to be the only variable affecting the lateral force developed.

Usable values of lateral force were developed by the full eyelid type of device with reasonably small losses in thrust and weight flow. Somewhat larger values of lateral force were developed by injecting a secondary flow normal to the primary jet, but for the conditions of these tests the losses in thrust and weight flow were large. Relatively good agreement with other investigations was obtained for several of the devices. The agreement of the present results with those of one of these investigations made with larger-scale equipment indicates that Reynolds number may not be critical for these tests.

Inasmuch as the effects of external flow could influence the performance and other factors affecting the choice of a reaction control for a specific use, it would appear desirable to make further tests of the devices described in this report in the presence of external flow.

Langley Research Center,
National Aeronautics and Space Administration,
Langley Field, Va., November 17, 1958.

REFERENCES

1. Blackaby, James R.: An Investigation of the Effects of Jet-Outlet Cut-Off Angle on Thrust Direction and Body Pitching Moment. NACA TN 2379, 1951.

2. Valerino, Alfred S.: Static Investigation of Several Jet Deflectors for Longitudinal Control of an Aircraft. NACA RM E55D04, 1955.

3. Rowe, P.: Supersonic Jet Deflection. Part I. Methods of Jet Deflection and a Review of Previous Work. PDGW Rep./EMR/52/4 (Imperial College. Rep. JRL No. 24), British Ministry of Supply, Sept. 1952.

4. Eisenklam, P., and Rowe, P.: Supersonic Jet Deflection. Part II. Deflection by Inclined Tubular Extensions. PDGW Rep./EMR/52/5 (Imperial College. Rep. JRL No. 25), British Ministry of Supply, Sept. 1952.

5. Rowe, P.: Supersonic Jet Deflection. Part III. Deflection by Beveling the Nozzle Exit Plane. PDGW Rep./EMR/53/1 (Imperial College. Rep. JRL No. 26), British Ministry of Supply, Feb. 1953.

6. von Glahn, Uwe H.: Use of the Coanda Effect for Obtaining Jet Deflection and Lift With a Single Flat-Plate Deflection Surface. NACA TN 4272, 1958.

7. McArdle, Jack G.: Internal Characteristics and Performance of Several Jet Deflectors at Primary-Nozzle Pressure Ratios up to 3.0. NACA TN 4264, 1958.

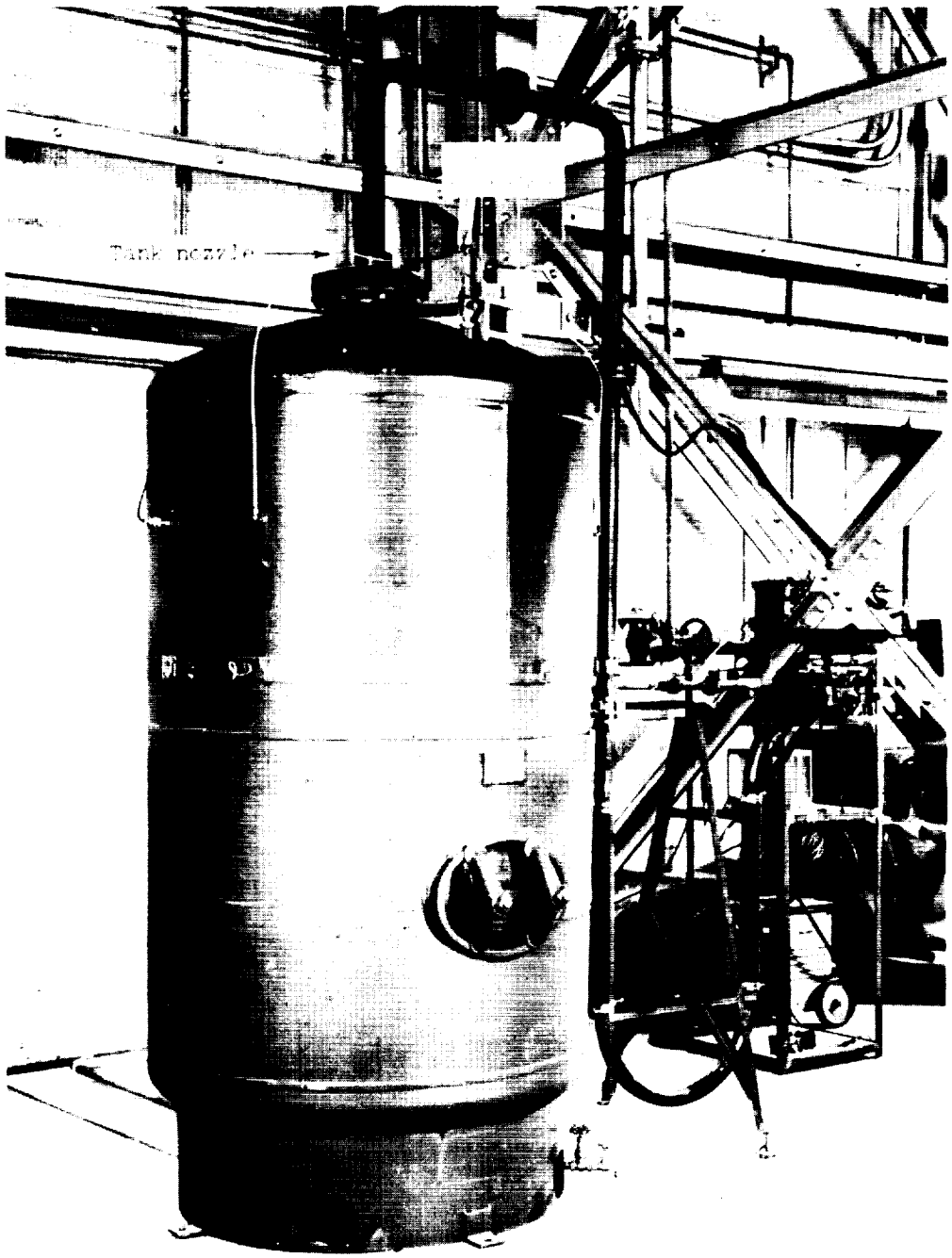

(a) Overall view of apparatus. L-91852.1

Figure 1.- Apparatus used in tests.

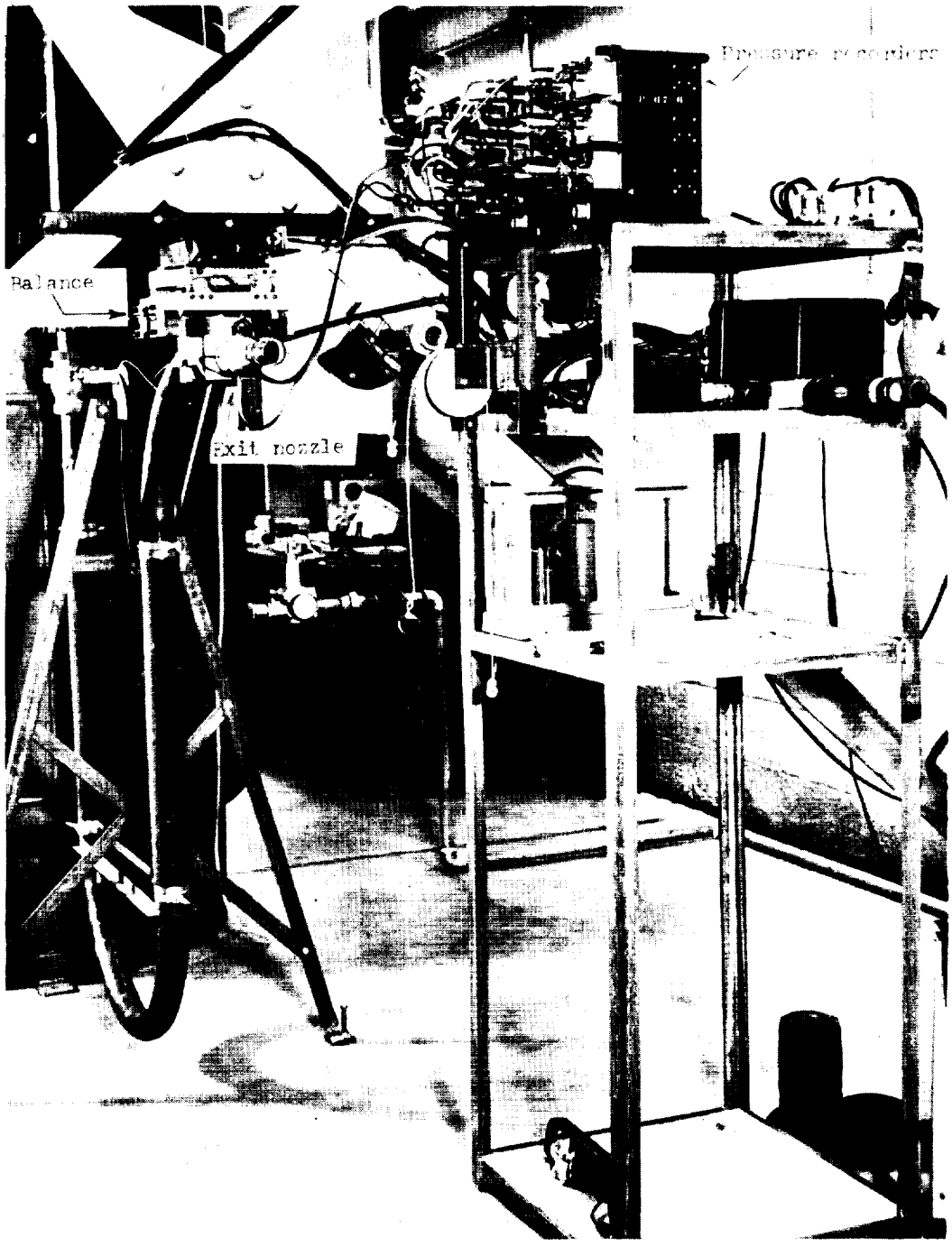

(b) Nozzle and instrumentation. L-91853.1

Figure 1.- Concluded.

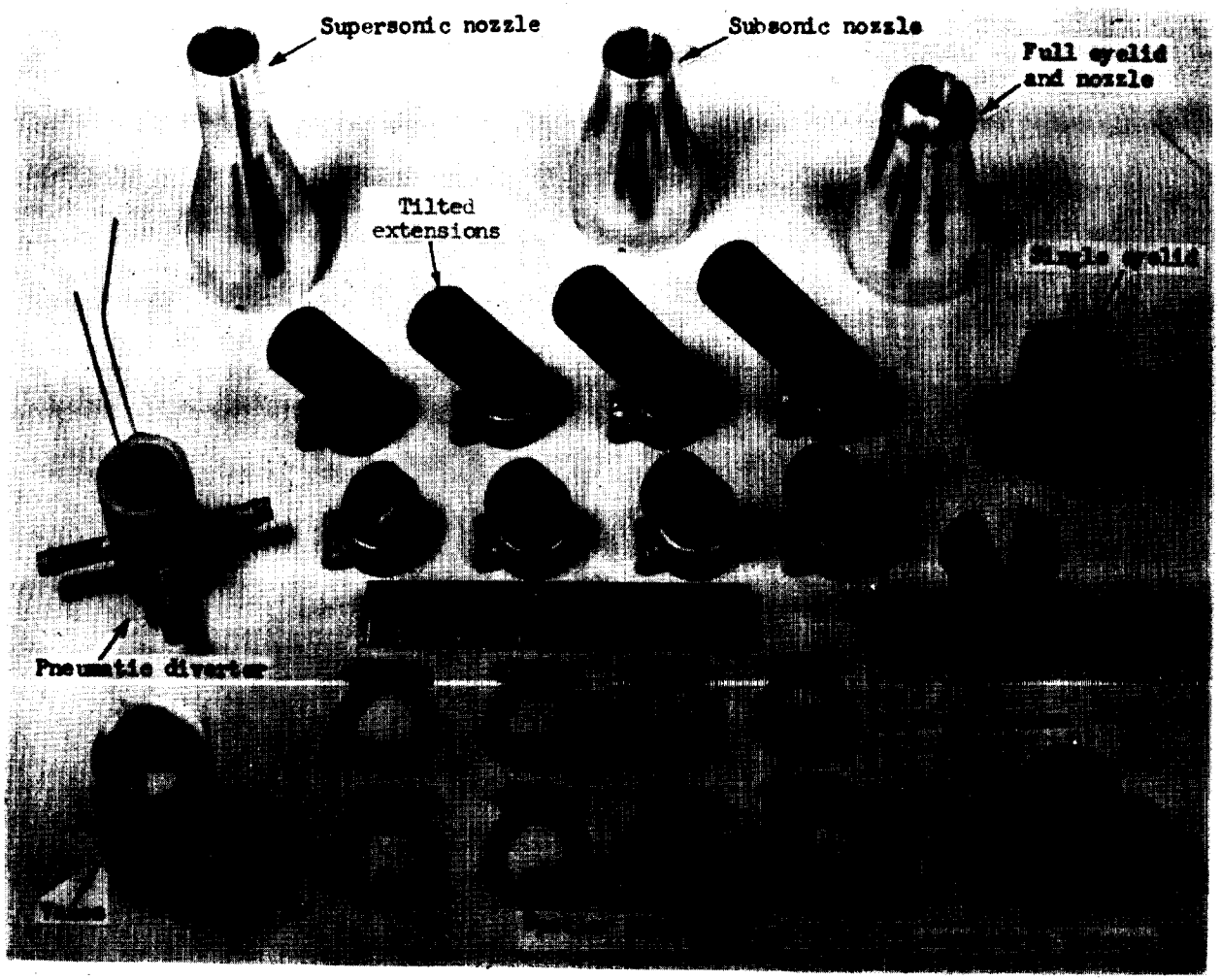

(a) Photograph of devices. L-91854.1

Figure 2.- Representative deflection devices tested.

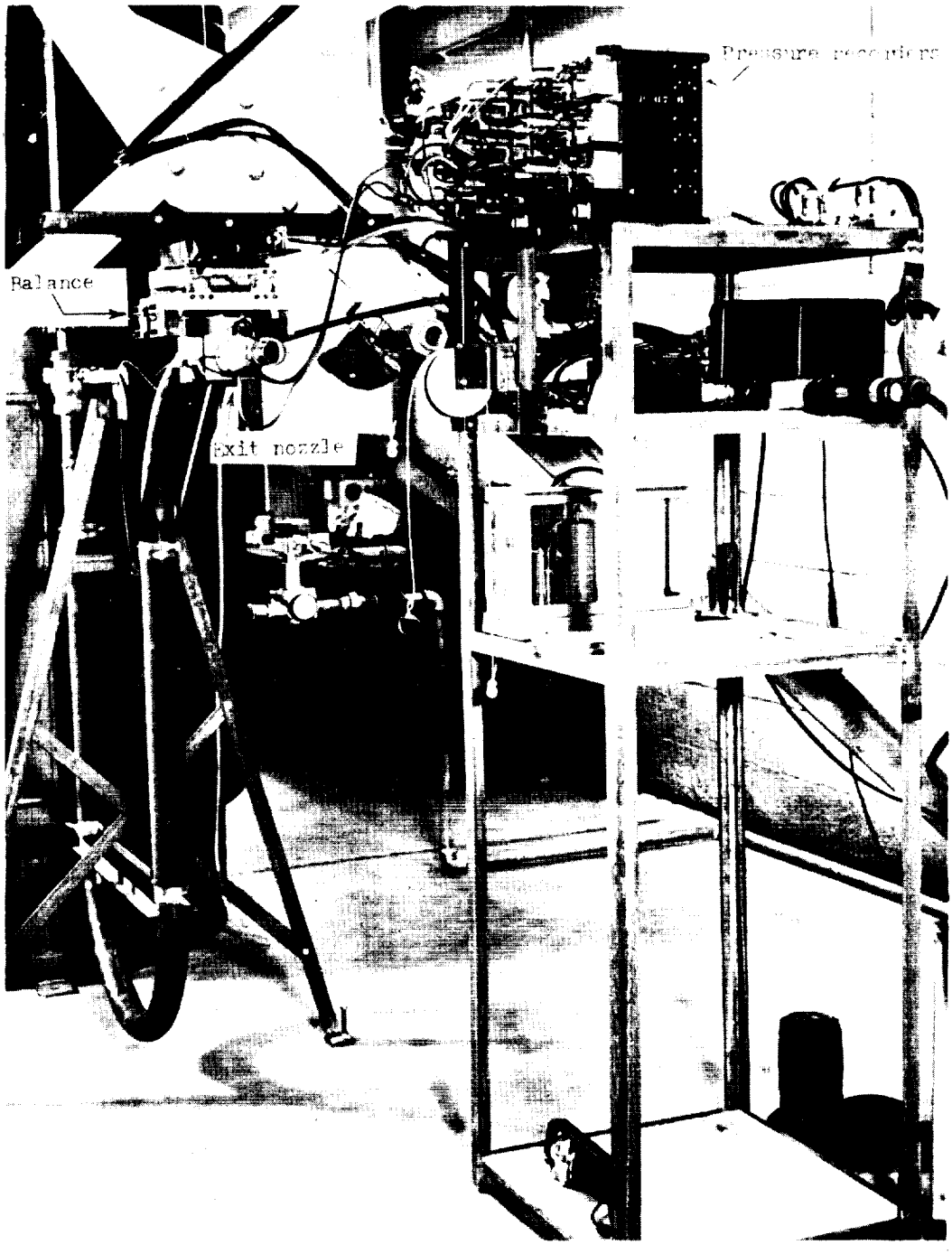

(b) Nozzle and instrumentation. L-91853.1

Figure 1.- Concluded.

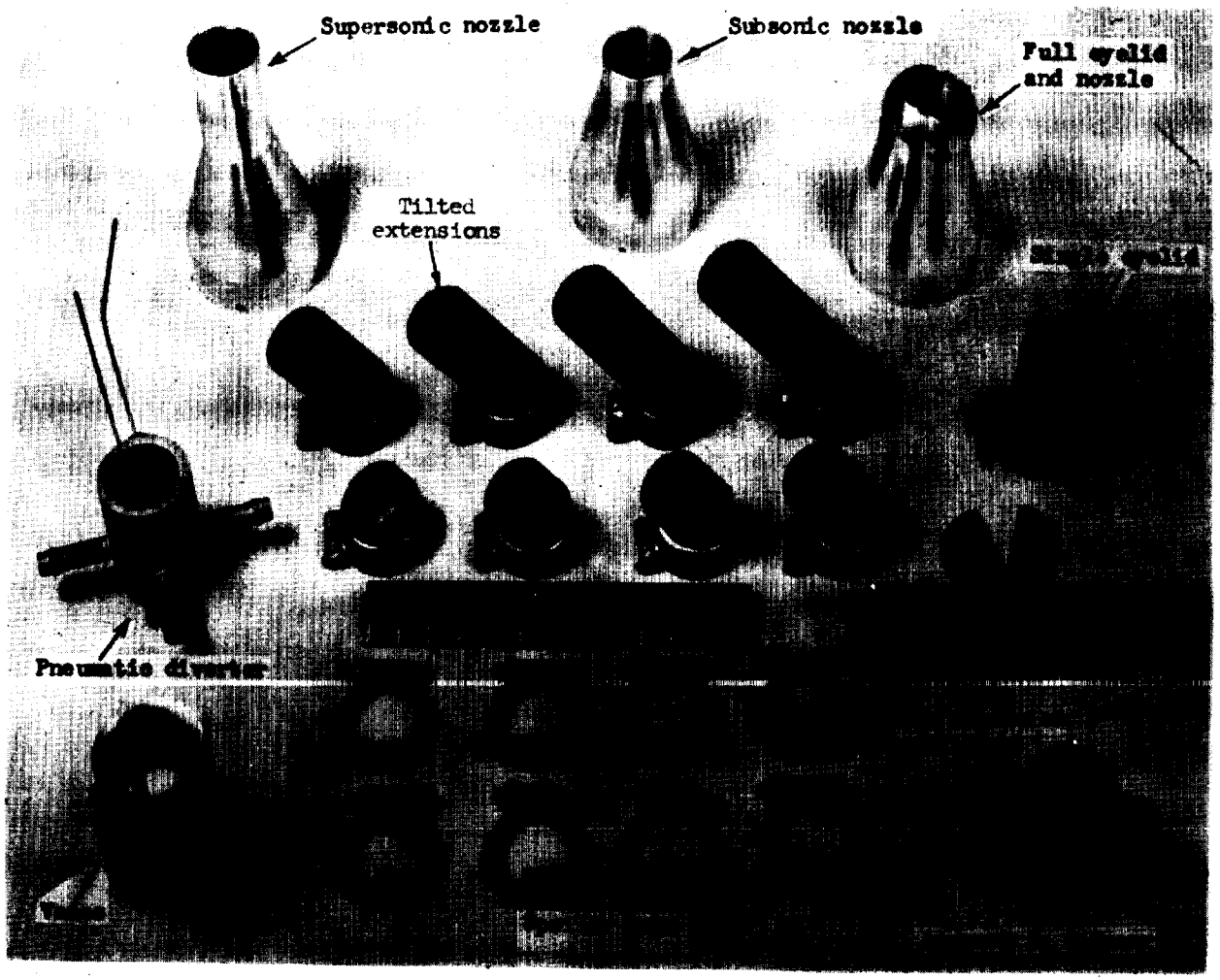

(a) Photograph of devices. L-91854.1

Figure 2.- Representative deflection devices tested.

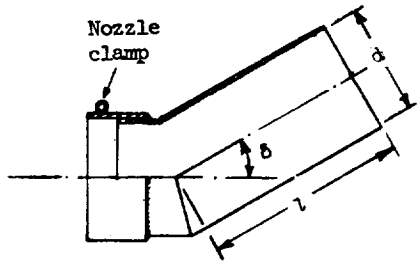

Tilted extension

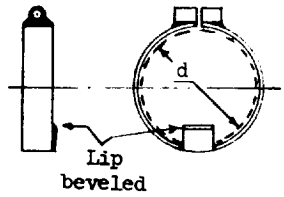

Spoiler tab

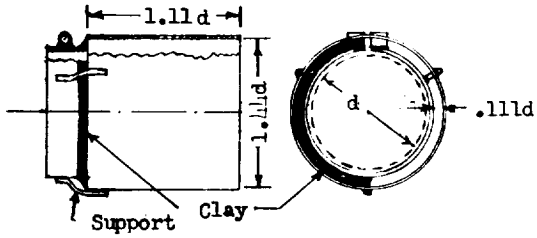

Asymmetric inducer

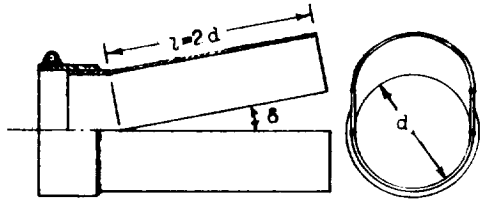

Split extension

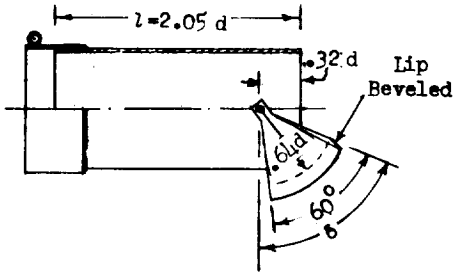

Single eyelid

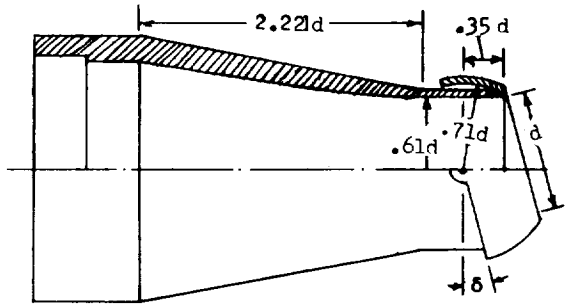

Full eyelid and nozzle

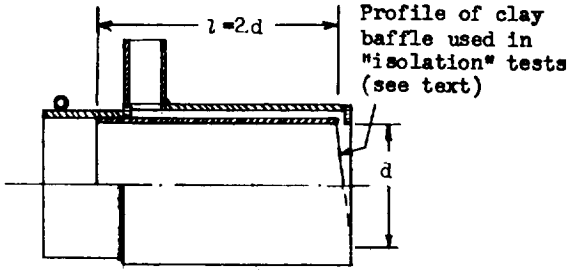

Pneumatic diverter

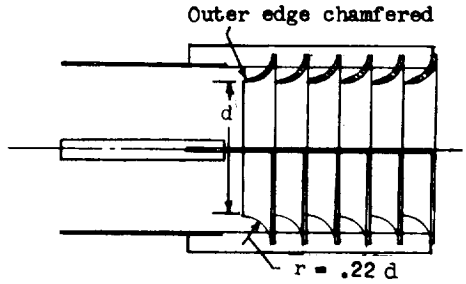

Pneumatic diverter vanes

(b) Sketches of devices.

Figure 2.- Continued.

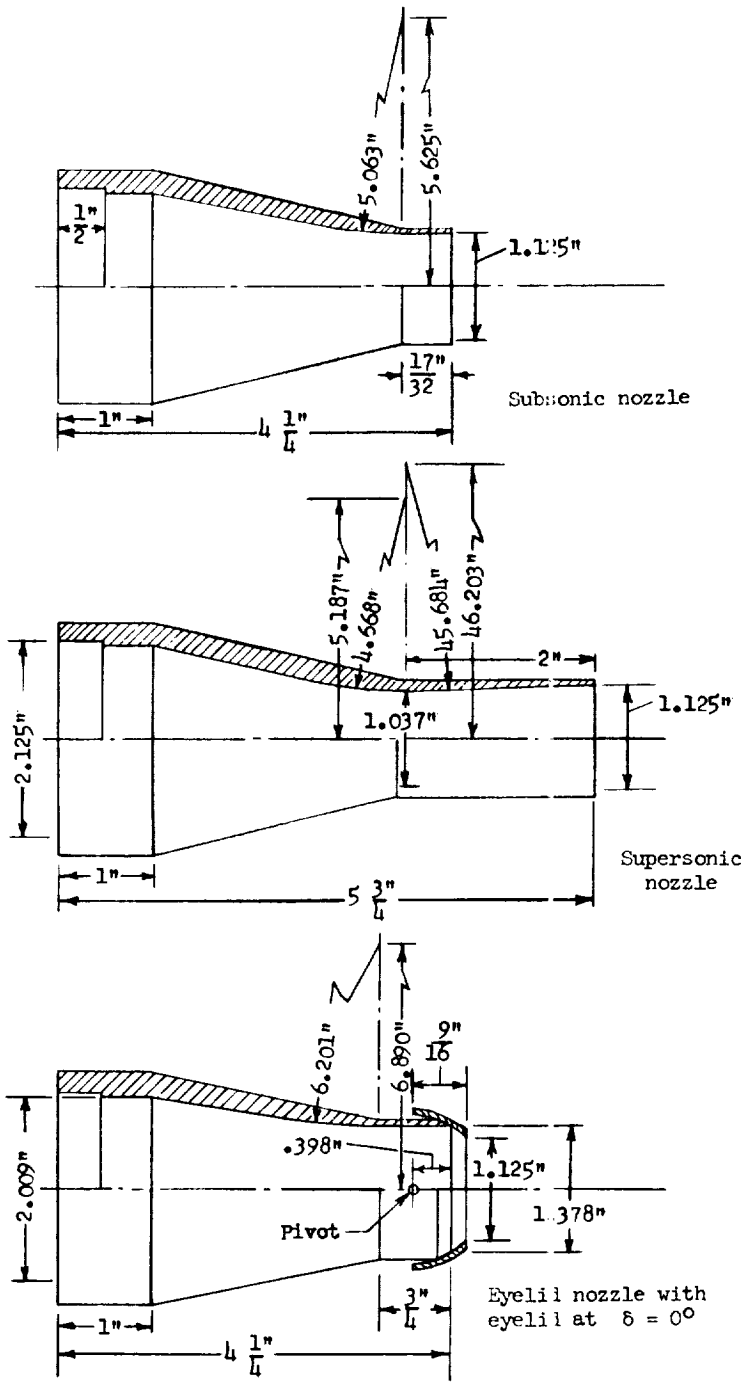

(c) Sketches of nozzles.

Figure 2.- Concluded.

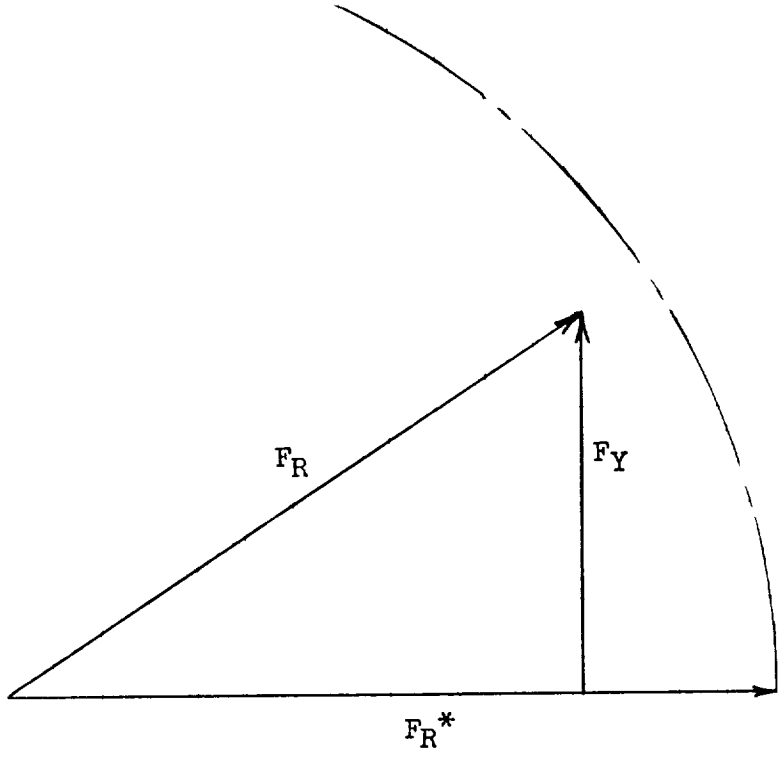

Figure 3.- Typical vector diagram of reaction control forces.

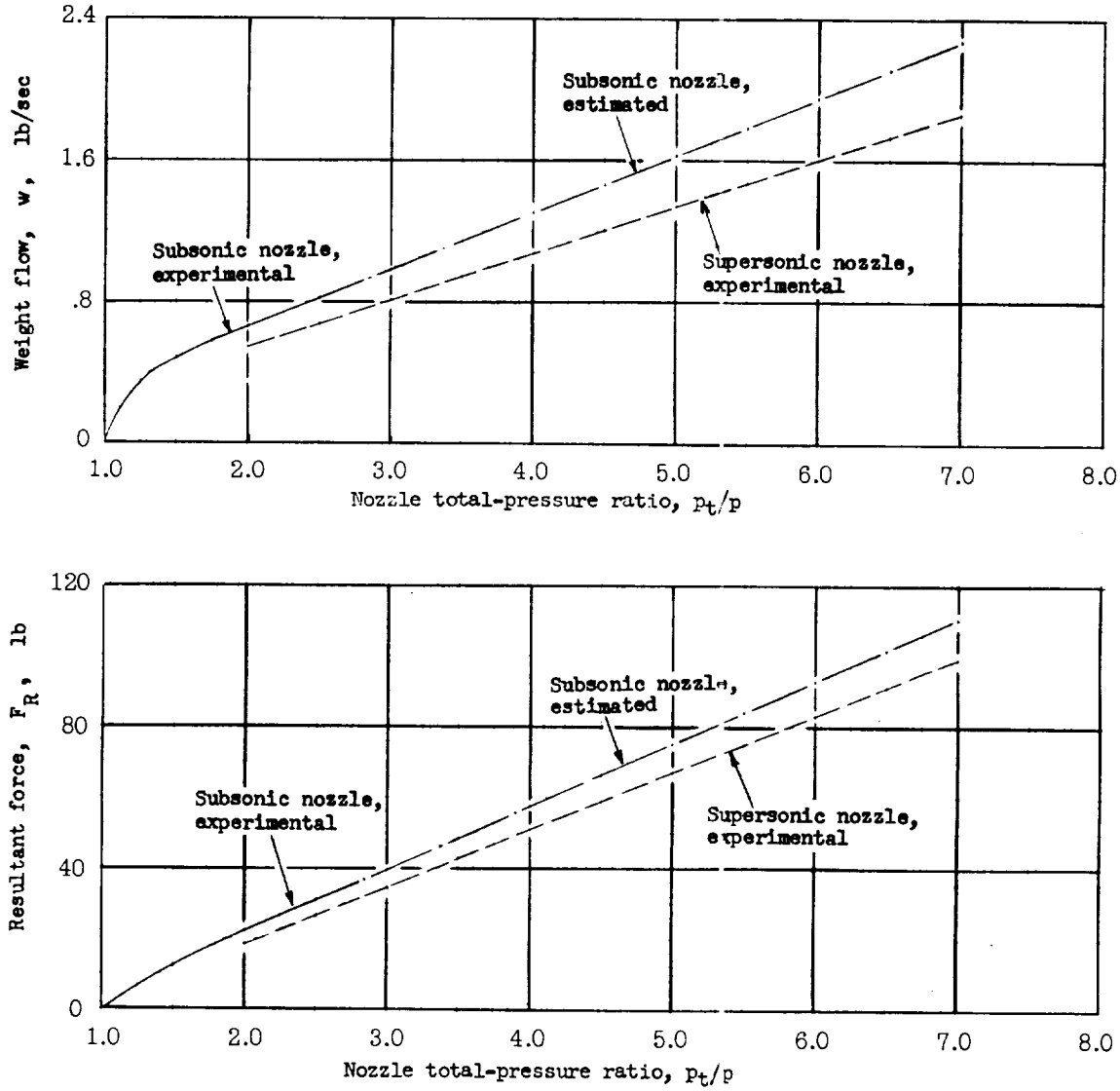

Figure 4.- Thrust and weight flow of undeflected jet.

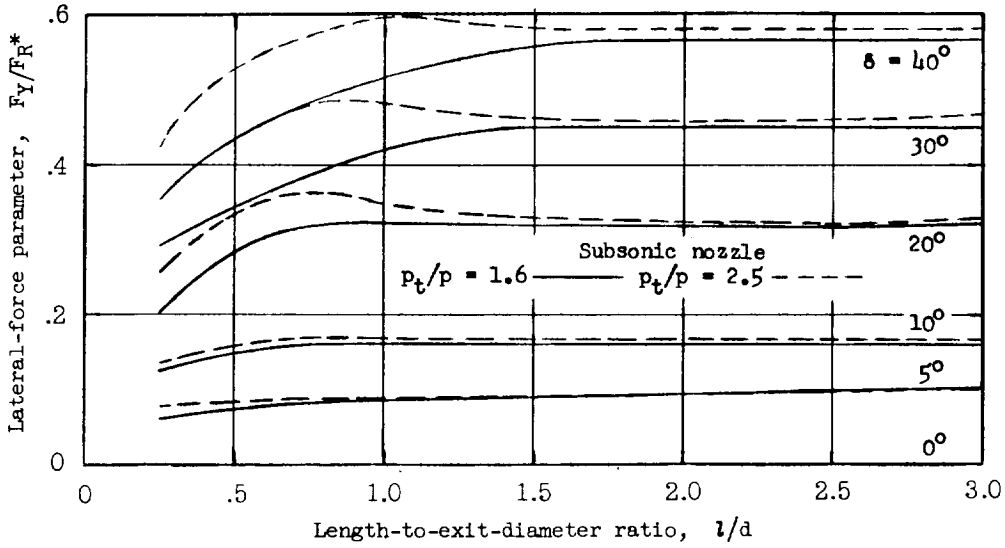

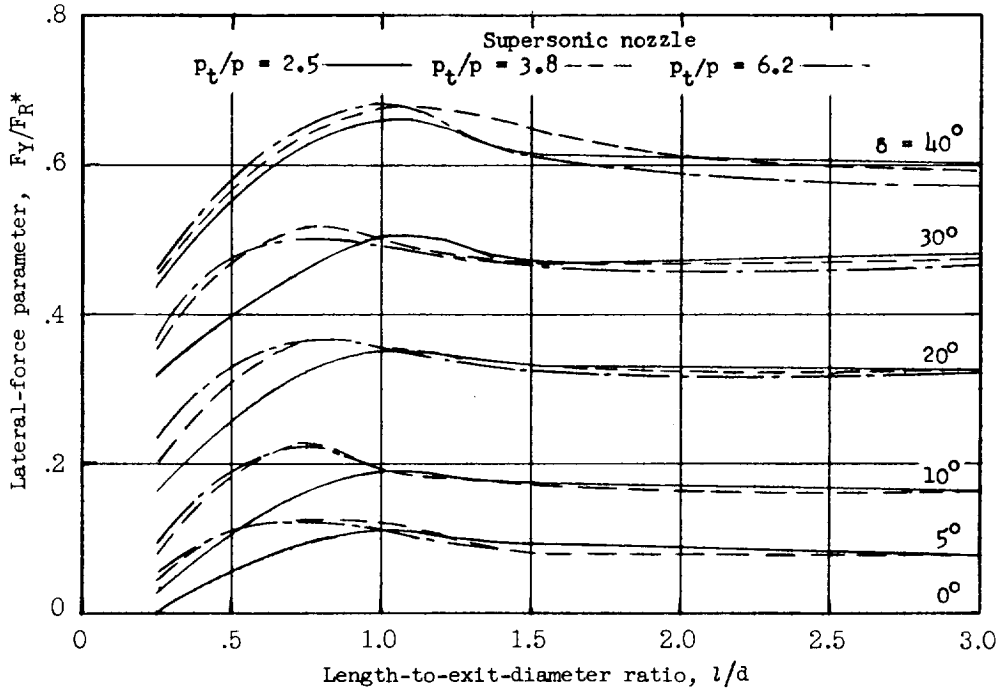

(a) Lateral-force parameter.

Figure 5.- Performance characteristics of tilted extensions.

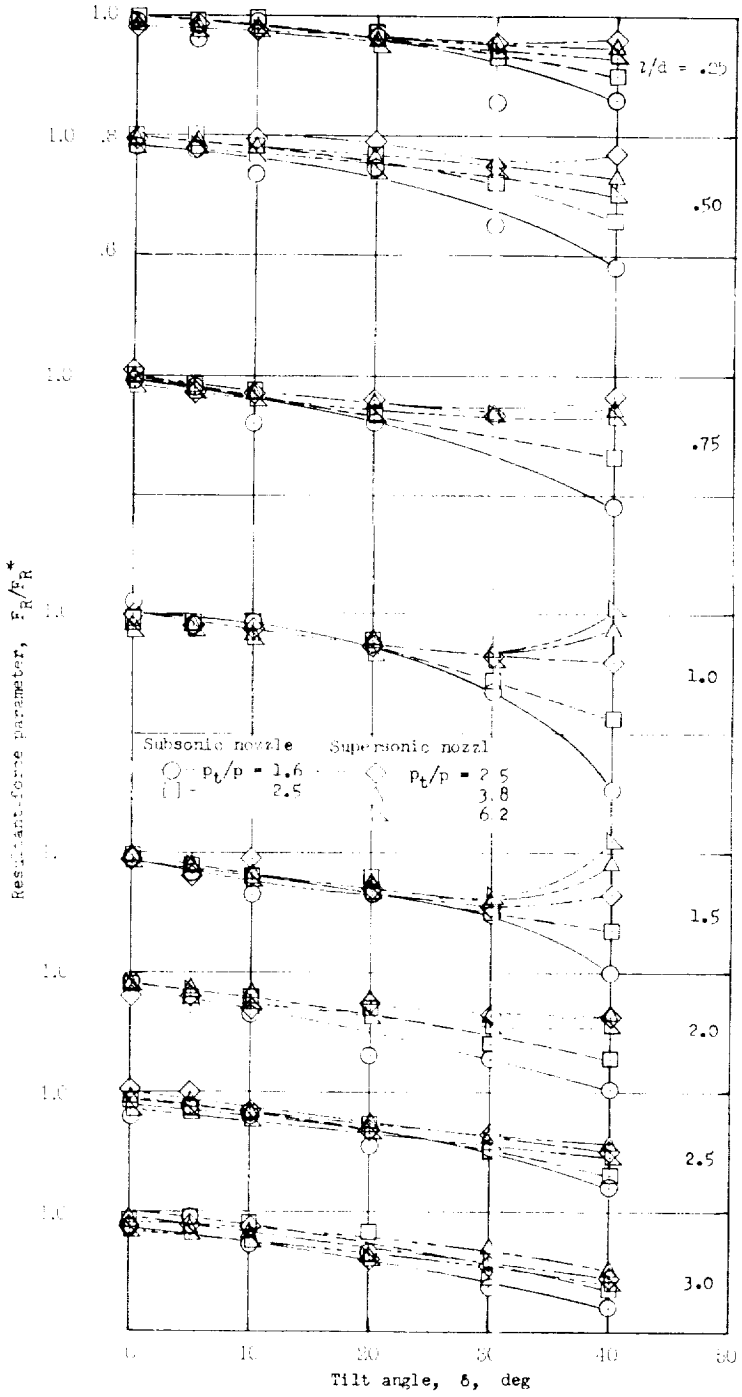

(b) Resultant-force parameter.

Figure 5.- Continued.

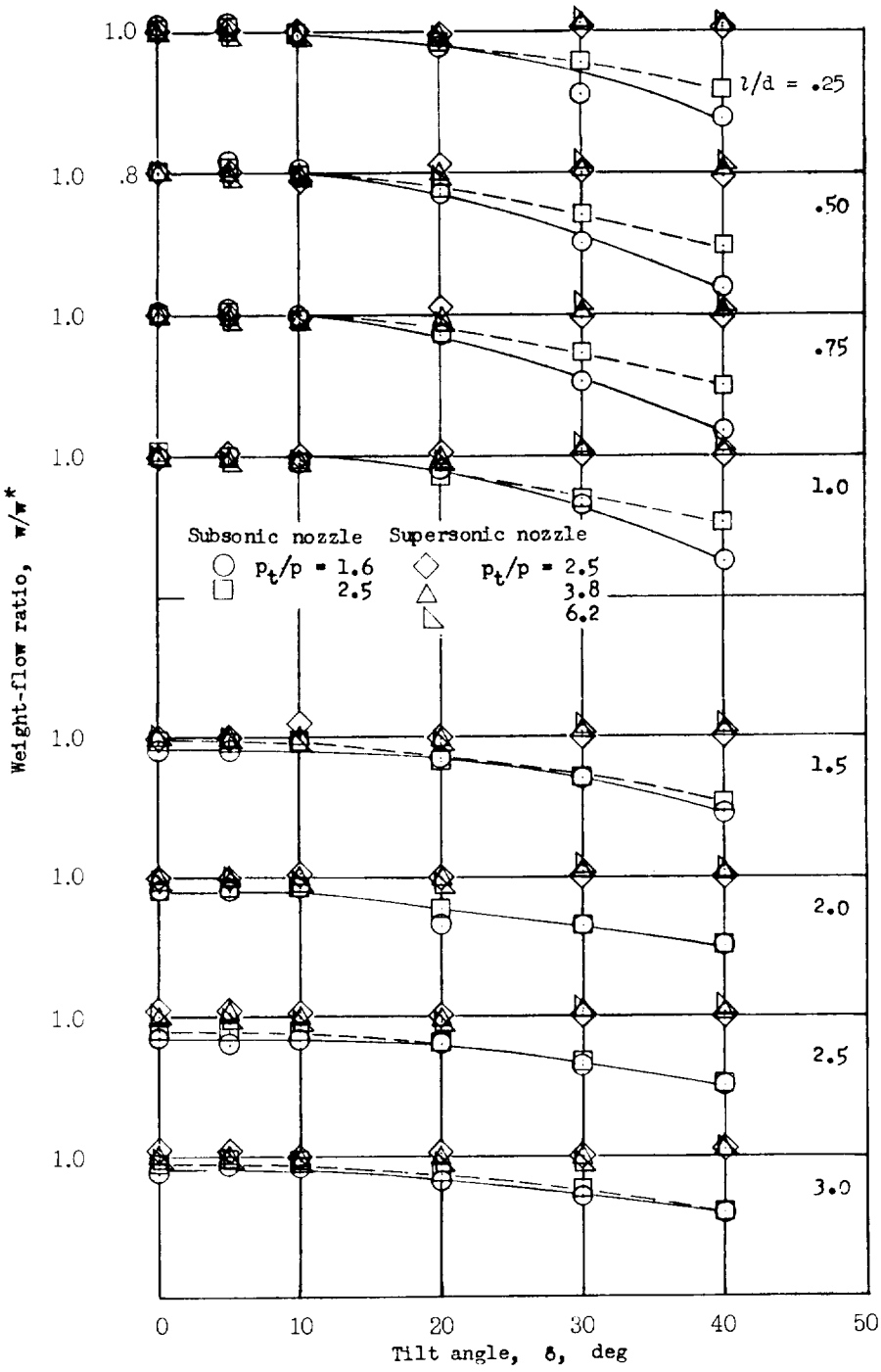

(c) Weight-flow ratio.

Figure 5.- Concluded.

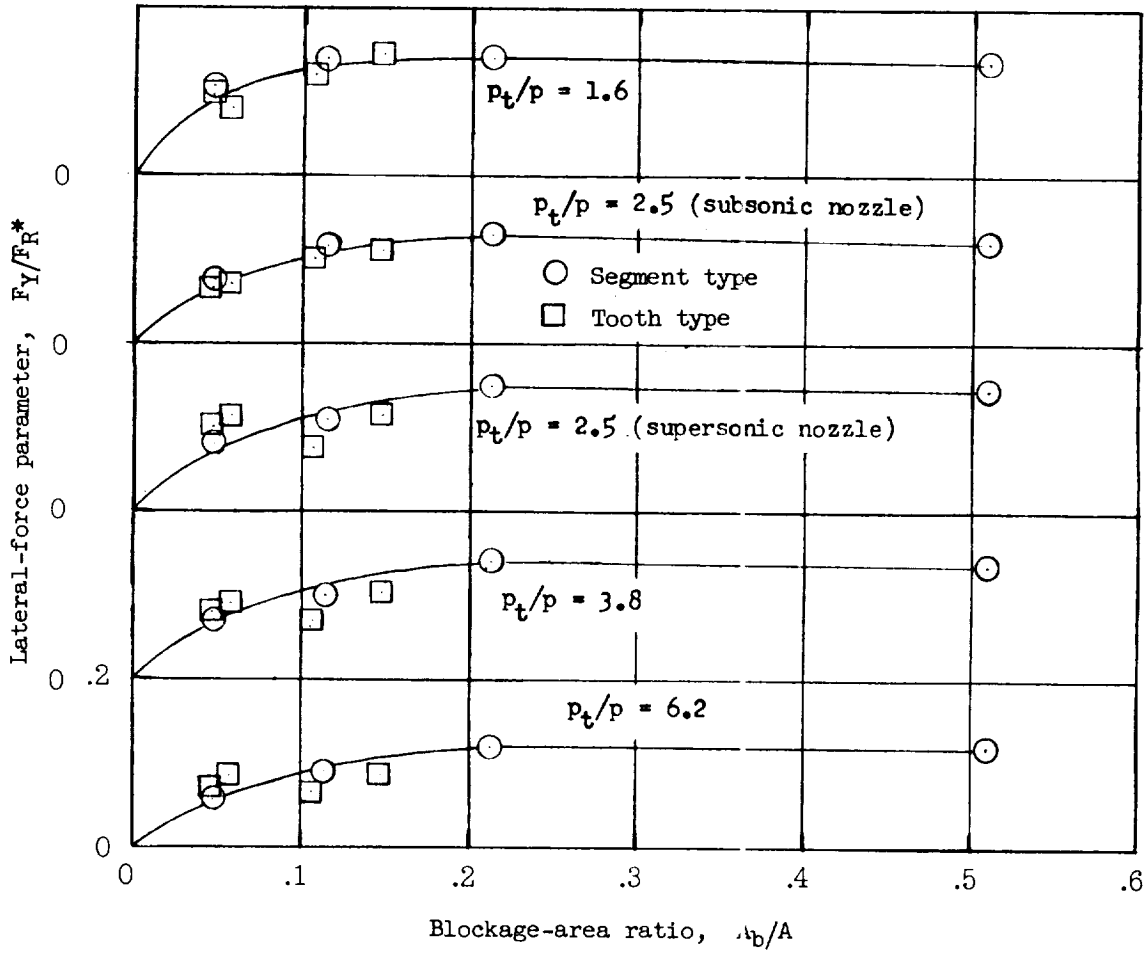

(a) Lateral-force parameter.

Figure 6.- Performance characteristics of spoiler tabs.

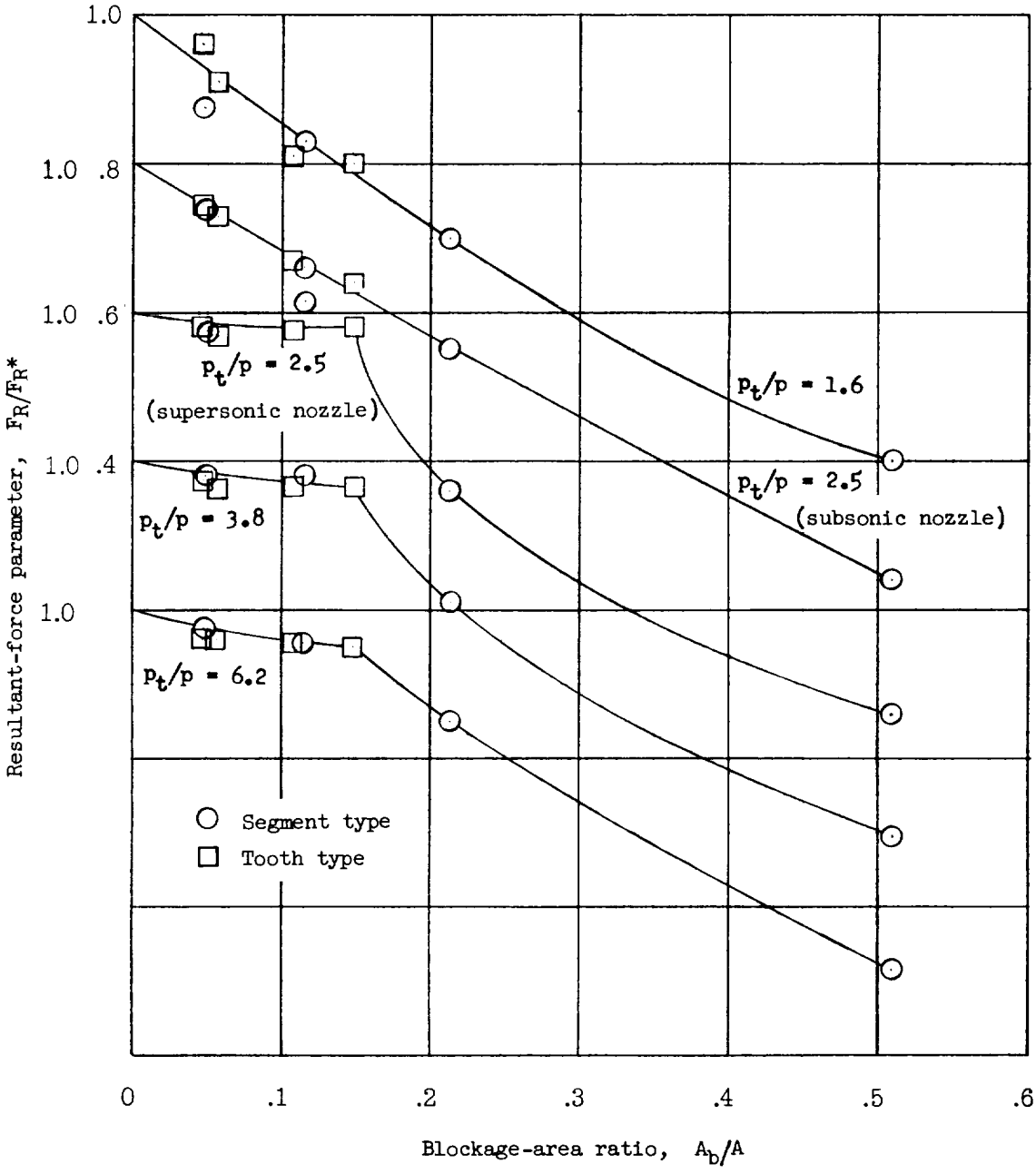

(b) Resultant-force parameter.

Figure 6.- Continued.

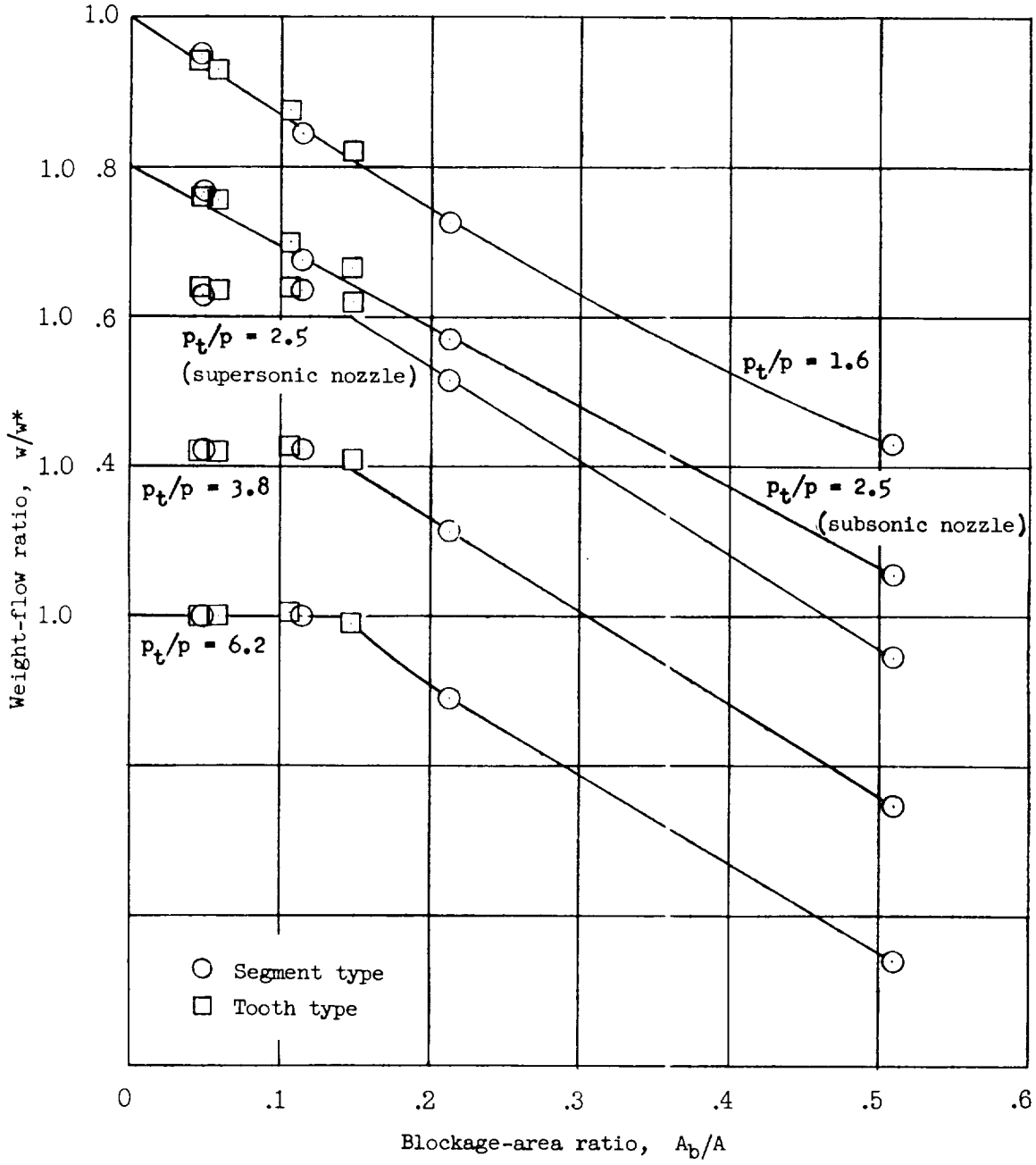

(c) Weight-flow ratio.

Figure 6.- Concluded.

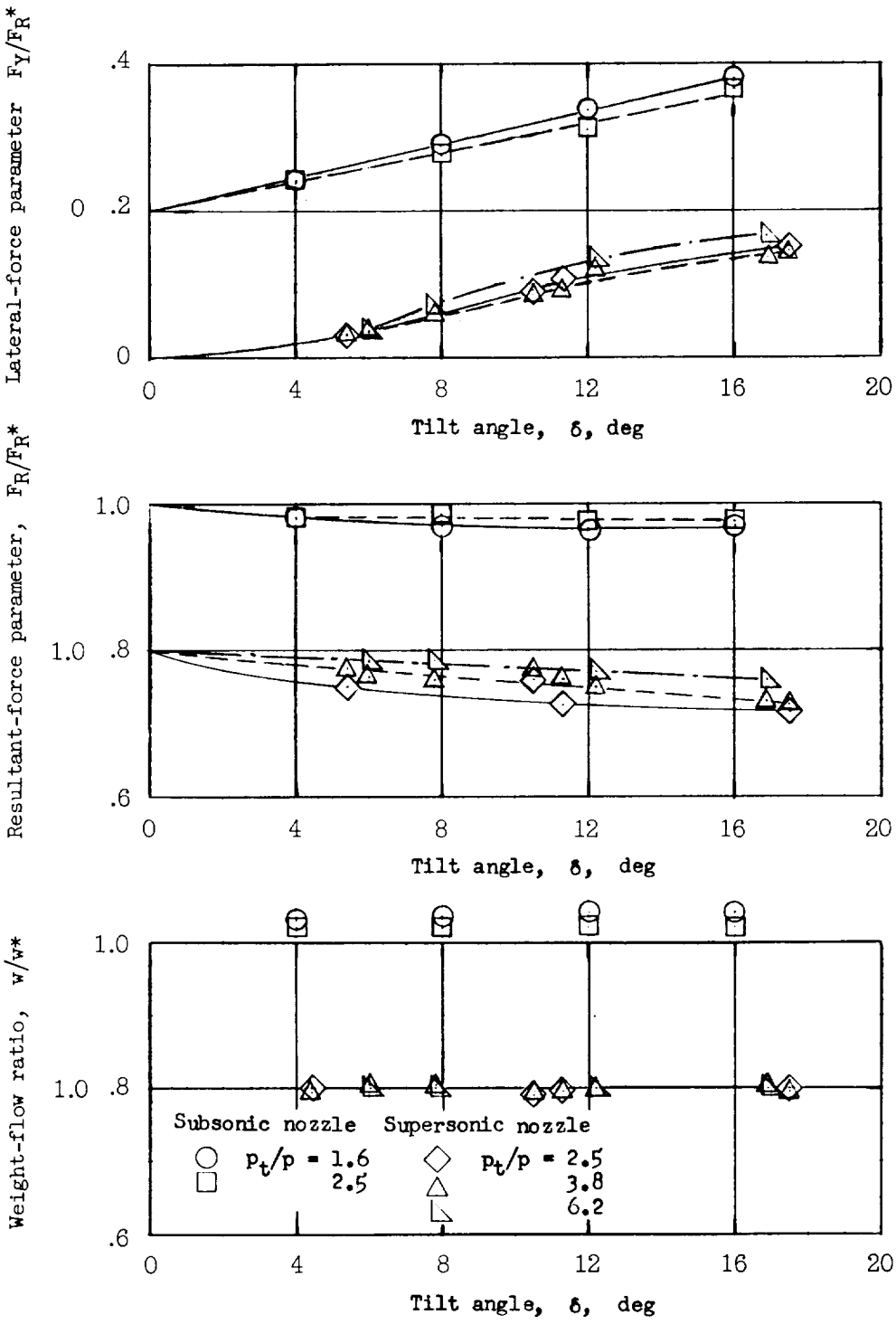

Figure 7.- Performance characteristics of the split extensions.

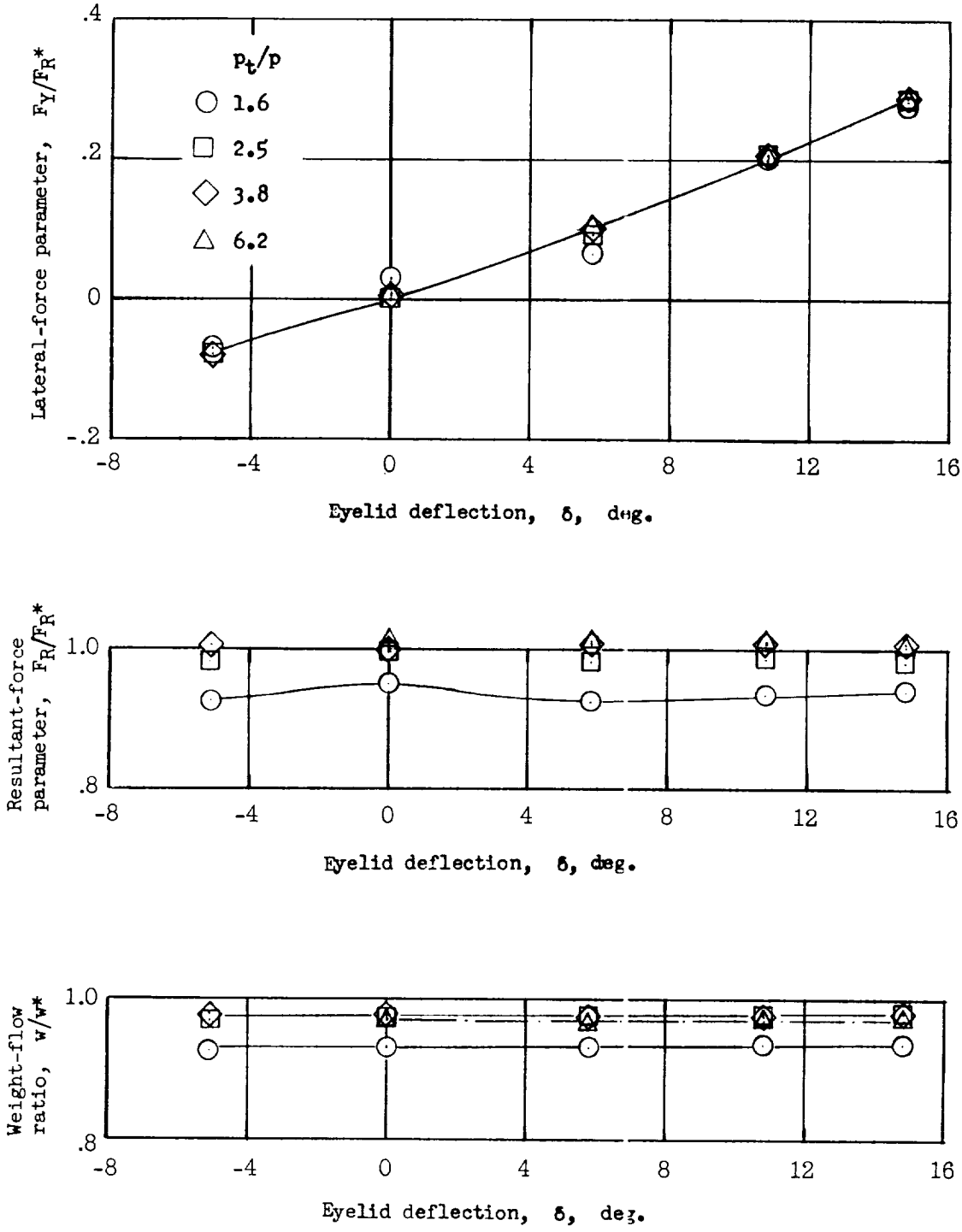

Figure 8.- Performance characteristics of the full eyelid.

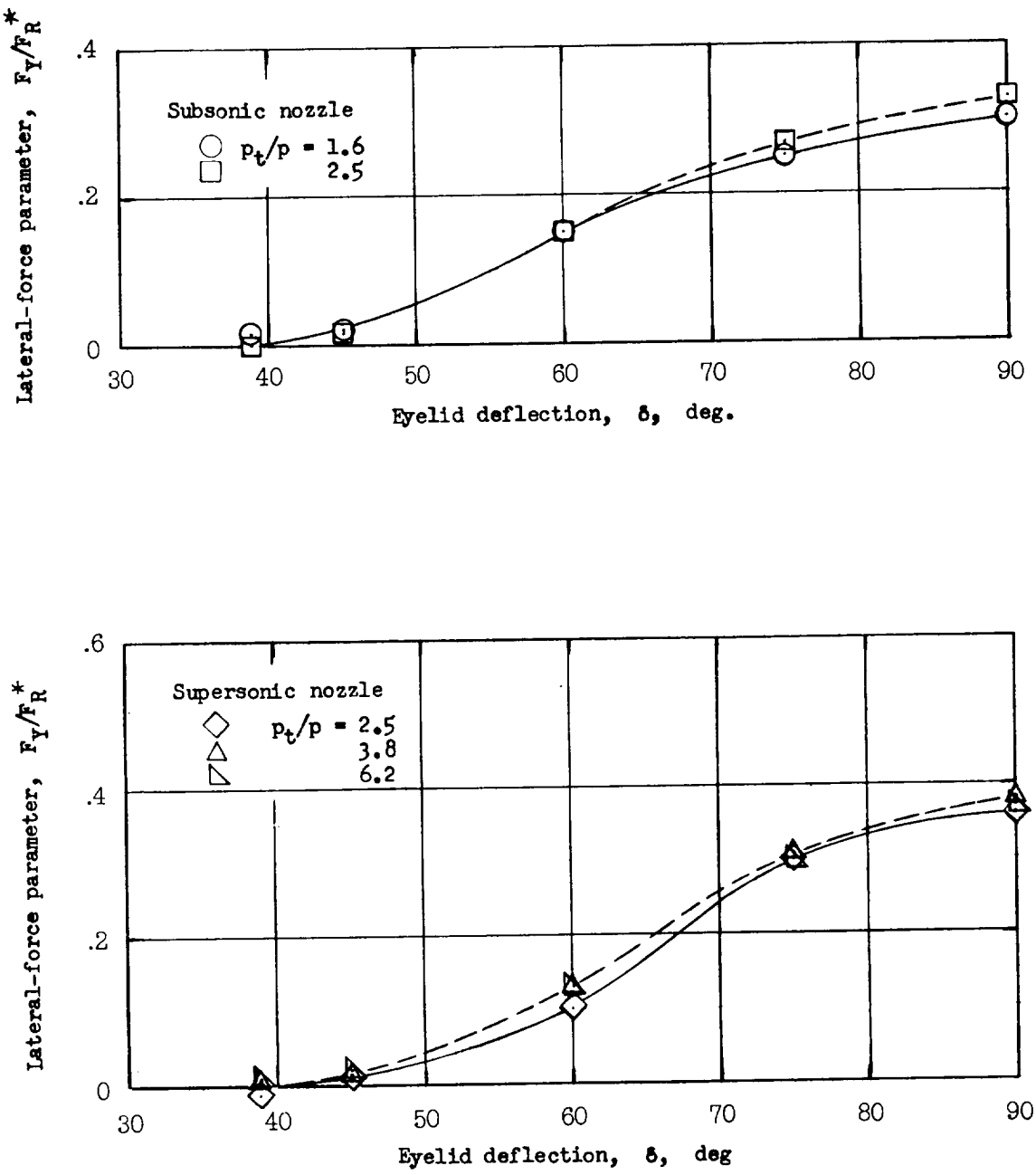

(a) Lateral-force parameter.

Figure 9.- Performance characteristics of the single eyelid.

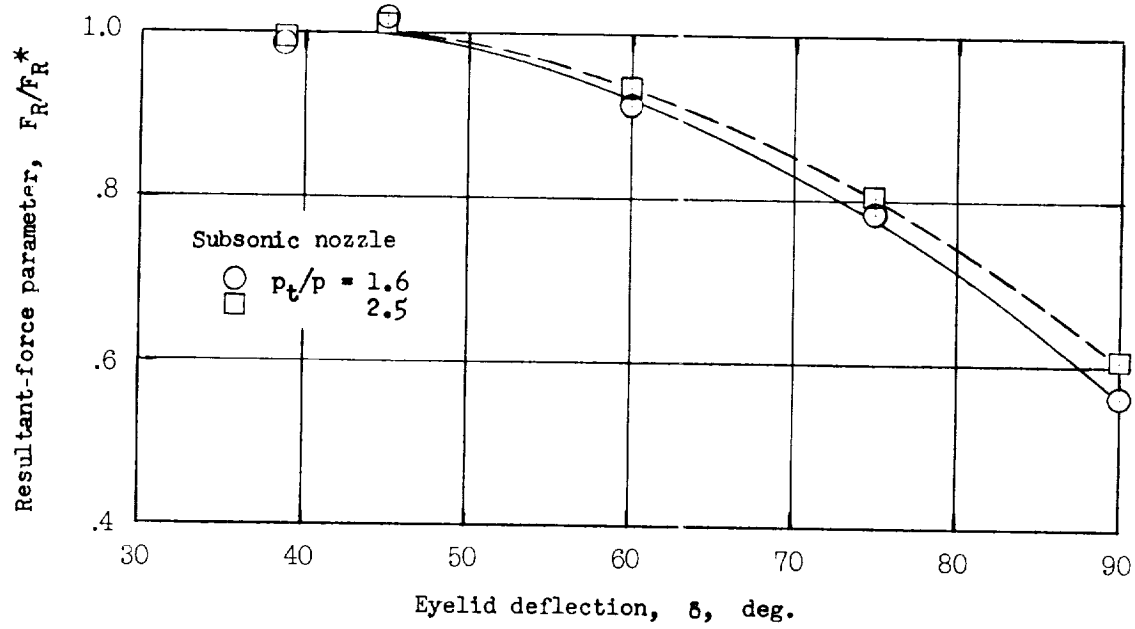

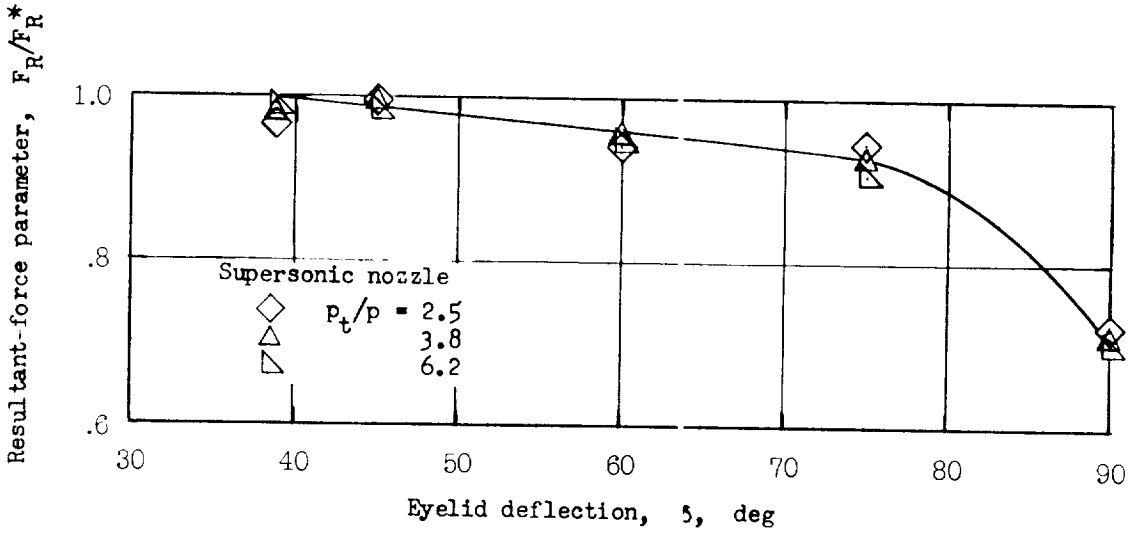

(b) Resultant-force parameter.

Figure 9.- Continued.

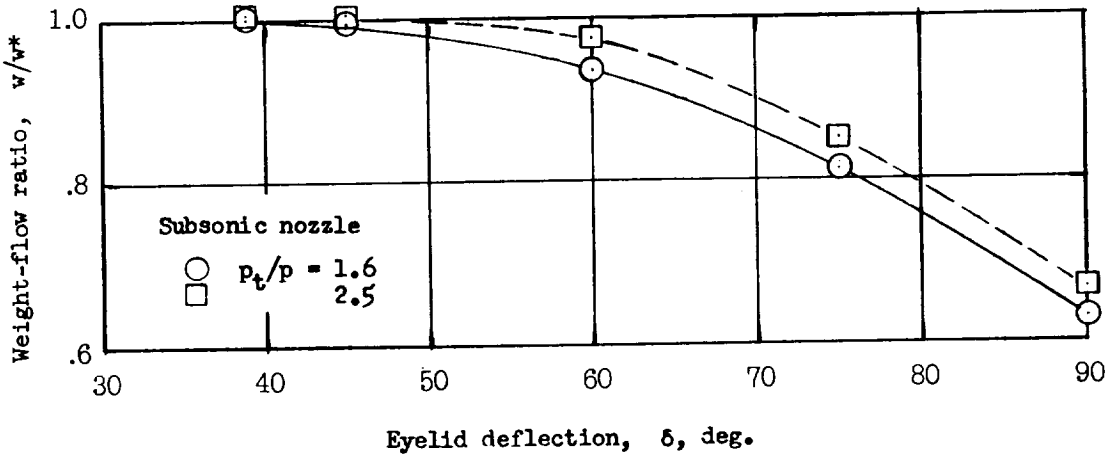

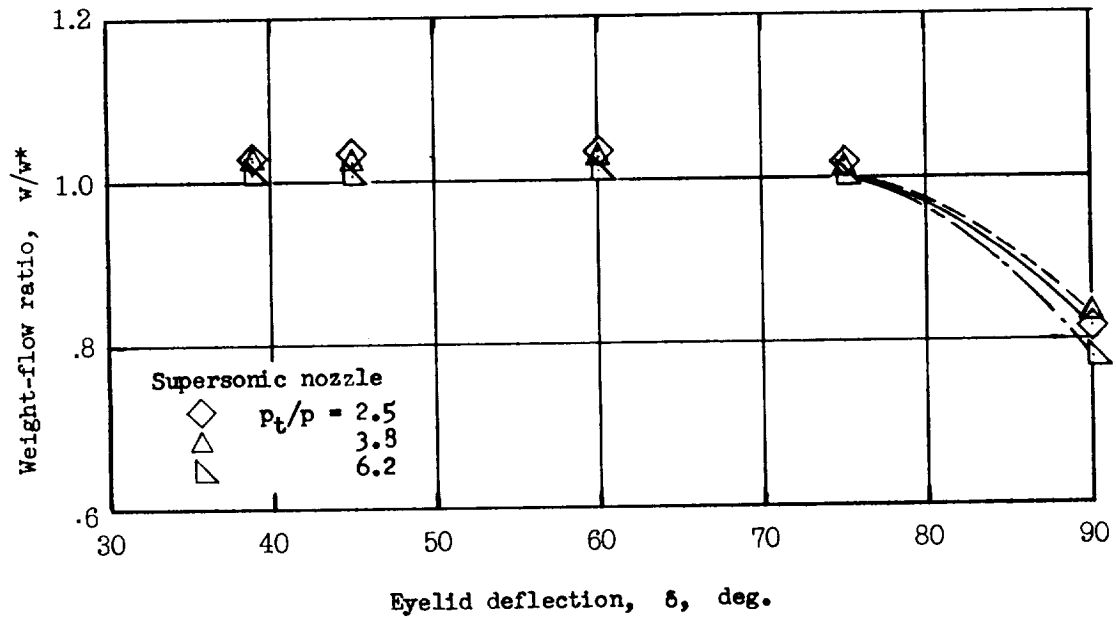

(c) Weight-flow ratio.

Figure 9.- Concluded.

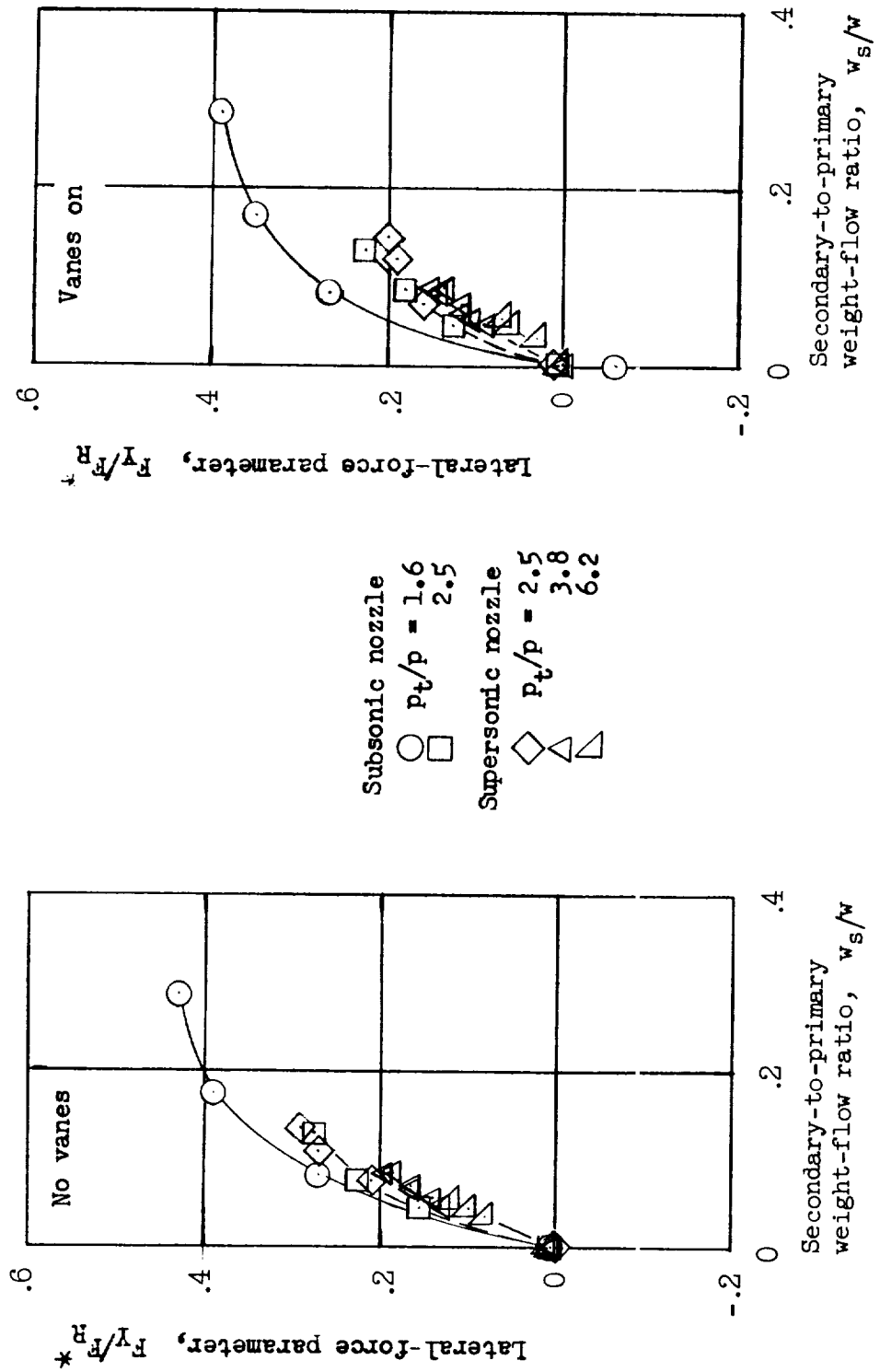

(a) Lateral-force parameter.

Figure 10.- Performance characteristics of the pneumatic diverter.

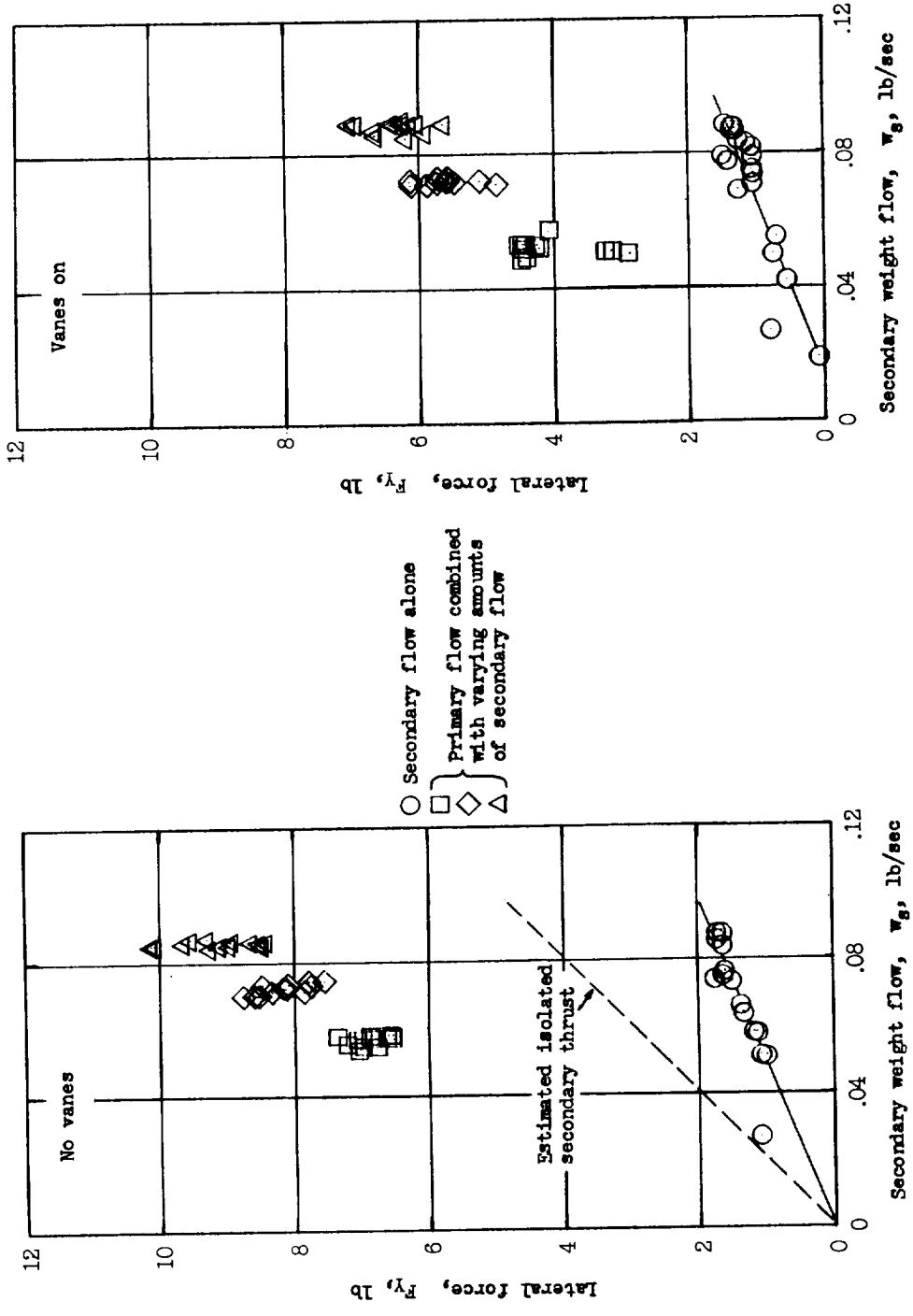

(b) Examples of the lateral forces developed by secondary flow alone and by combined primary and secondary flows. Supersonic nozzle p_t/p varying from 6.5 to 3.4 for primary flow.

Figure 10.- Continued.

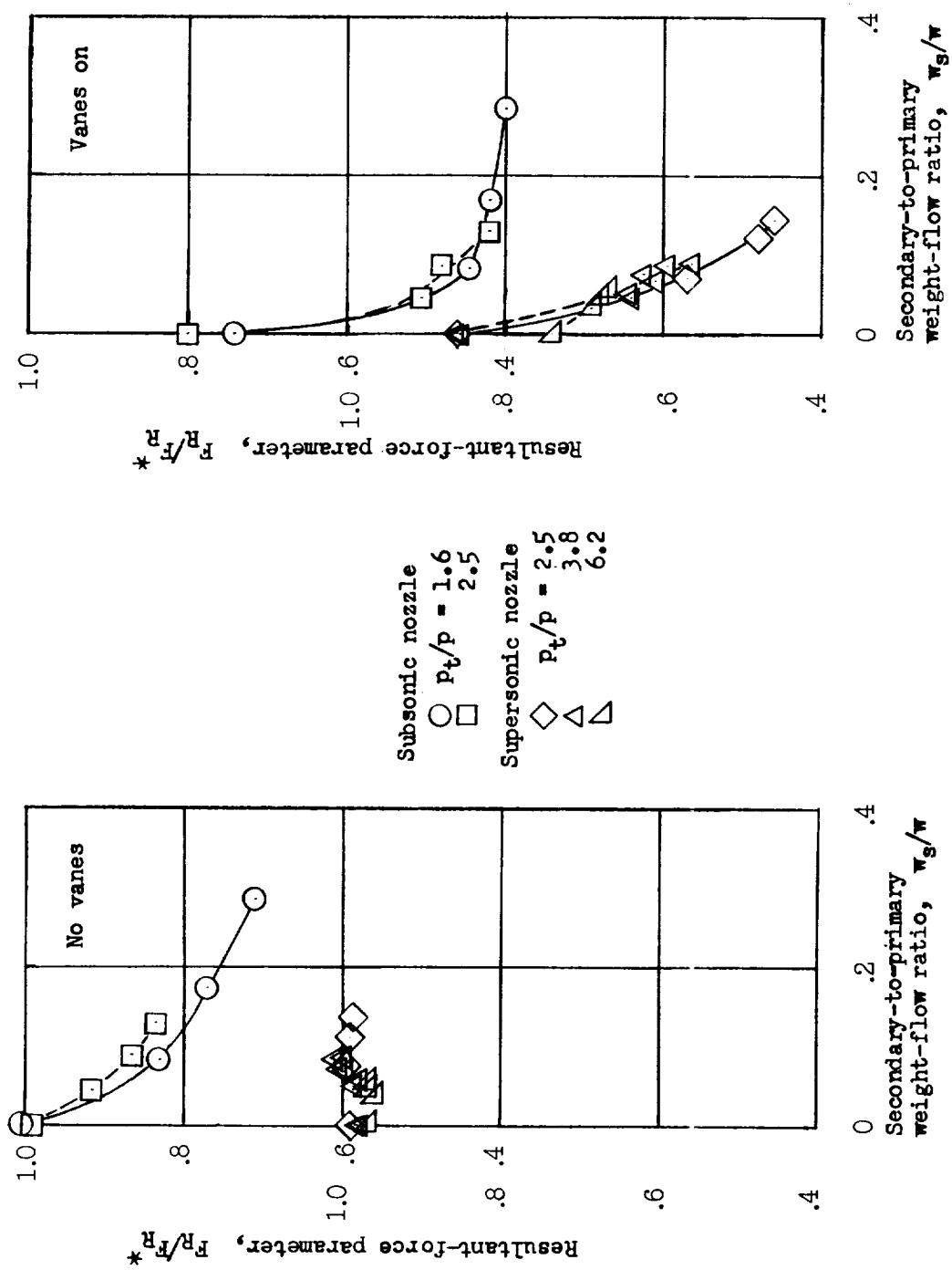

(c) Resultant-force parameter.

Figure 10.- Continued.

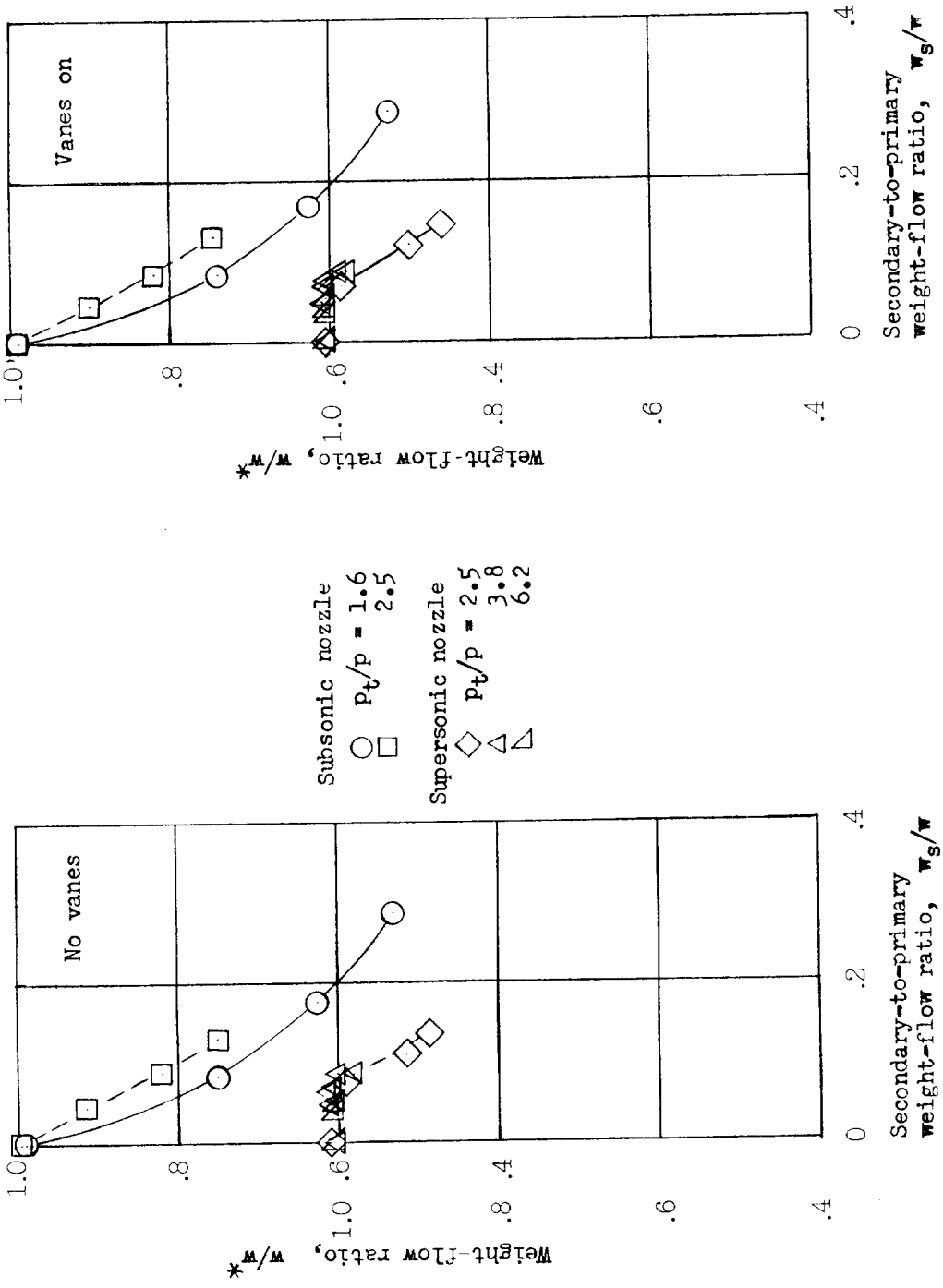

(d) Primary weight-flow ratio.

Figure 10.- Concluded.